Chemical Engineering Journal 456 (2023) 140968

Contents lists available at ScienceDirect

Chemical Engineering Journal

journal homepage: www.elsevier.com/locate/cej

Review

Geomechanical challenges during geological CO_2 storage: A review

Youngsoo Song [a], Sungjun Jun [a], Yoonsu Na [a], Kyuhyun Kim [a], Youngho Jang [b,*], Jihoon Wang [a,c,*]

[a] Department of Earth Resources and Environmental Engineering, Hanyang University, Seoul 04763, Republic of Korea
[b] R&D Planning and Evaluation Division, Korea Institute of Energy Technology Evaluation and Planning, Seoul 06175, Republic of Korea
[c] Petroleum and Natural Gas Engineering Department, New Mexico Institute of Mining and Technology, Socorro, NM 87801, USA

A B S T R A C T

Carbon capture and sequestration (CCS) method is the only viable method for reducing massive amount of carbon dioxide (CO_2) from the atmosphere to prevent the subsequent environmental and health threats. However, the process is accompanied with geomechanical risks due to the unavoidable pore pressure buildup, such as caprock failure, reactivation of existing faults, poroelastic response of rock and well integrity loss. Not only may the risks lead to undesirable environmental concerns such as CO_2 leakage to the surface, induced seismicity, and surface uplift, but it also would disturb achieving the public's consensus on the CCS process. In this paper, we present an overview of possible geomechanical risks during CCS. We also review the mechanisms and theories of possible geomechanical risks during the CCS and the relevant precedent studies are introduced and described. This study would facilitate understanding the potential geomechanical risks during the CCS and establishing the optimal design of the CCS process to achieve the public acceptance. Some challenges related to handling the geomechanical risks during the CCS are also discussed.

1. Introduction

According to the Paris agreement, 197 countries have reached for the 'low greenhouse gas emissions development' [1], which restricts the greenhouse gas emission of the signees to achieve the global average temperature rise within 1.5 °C above pre-industrial levels. The anthropogenic CO_2 emission will be reduced by the carbon capture, utilization and storage (CCUS) technologies. When the carbon capture and sequestration (CCS), also known as the geological carbon storage (GCS), is adopted, CO_2 is injected and stored in a targeted geologic structure such as depleted hydrocarbon reservoirs, saline aquifers, and underground caverns [2,3]. CCS is the most feasible way to remove and sequestrate the massive amount of CO_2.

According to the sustainable development scenario projected by International Energy Agency (IEA), at least 650 megatons of the anthropogenic CO_2 is required to be stored annually by 2030 to meet the emission goals. The CO_2 storage capacity of the current large commercial CCS projects is approximately 40 megatons per year, which is only 6 % of the desired amount [4]. In the same manner, the South Korea government plans to reduce the CO_2 emission by 40 % business as usual (BAU) in 2030 and achieve the net-zero by 2050. The amount of CO_2 sequestrated by the CCS process is expected as at least 55 megatons, 69 % of the total CO_2 reduction until 2050 [5]. One of the target geologic structure is the depleted Donghae gas reservoir in East Sea, which is planned to be repurposed for the CO_2 storage, where 0.4 megaton of CO_2 per year are expected to be geologically stored from 2025 [6].

When CO_2 is injected and stored into an underground geological structure, the pore pressure buildup is unavoidable. The change of the pore pressure redistributes the stress status and induces the poroelastic responses at the caprock and target formation [7–10]. If severe, it may lead to geomechanical hazards such as leakage of the injected CO_2, surface uplift, and induced seismicity, which are major environmental concerns during the CCS project. In addition, the well integrity should be considered because the injected CO_2 could be leaked through any component of the well what was designed to be used as the flowing path. Uncontrolled release of injected fluid can shorten life cycle of the well and it may lead to CO_2 leakage. Therefore, establishment of the optimal CCS design considering the geomechanical risks is important to perform the environmentally safe project and to achieve the public acceptance [11].

There are geomechanical risks during a CCS process, but investigations of causes, mechanisms and post-analysis methods have not yet been conducted [12]. In this paper, geomechanical risks potentially caused by the pore pressure buildup due to the CO_2 injection will be

* Corresponding authors at: Department of Earth Resources and Environmental Engineering, Hanyang University, Seoul 04763, Republic of Korea & Petroleum and Natural Gas Engineering Department, New Mexico Institute of Mining and Technology, Socorro, NM 87801, USA (J. Wang); R&D Planning and Evaluation Division, Korea Institute of Energy Technology Evaluation and Planning, Seoul 06175, Republic of Korea (Y. Jang).

E-mail addresses: jangyh@ketep.re.kr (Y. Jang), jihoonwang@hanyang.ac.kr (J. Wang).

https://doi.org/10.1016/j.cej.2022.140968
Received 9 December 2022; Accepted 12 December 2022
Available online 17 December 2022
1385-8947/

reviewed. We also provide the key principles to integrated geomechanical analysis for the optimal CCS design. The fundamentals are described with related precedent studies focusing on both computational and experimental approaches. Moreover, field scale applications of the possible environmental and health concerns are introduced. In Section 2, the overall geomechanical risks and its mechanisms are briefly described. The following sections focus on the mechanisms, theories and analysis methods based on the relevant studies. The research history and field scale observations reviewed in this study provide important fundamentals of the potential geomechanical risks that may occur during a CCS project. In addition, the paper suggests important insights of the geomechanical risks for establishment of the optimal injection strategies during the CCS to prevent the environmental hazards.

2. Possible geomechanical risks during the CCS project

When a CCS project is performed, a certain amount of CO_2 is injected and stored to meet the goal, which causes unavoidable pore pressure buildup. The potential geomechanical risks caused by the pore pressure buildup are summarized in Fig. 1. Although there is a specific desirable injection rate, it depends on the injectivity of the target reservoir. If the rate is too high, the pressure at the downhole can exceed the fracture pressure and can induce a tensile fracture. The well stimulation methods such as the hydraulic fracturing and acidizing can be a solution by enhancing the permeability of the near-wellbore region. On the other hand, the poroelastic response of the formation is unavoidable once the pore pressure of the reservoir changes. If the pore pressure buildup is severe, the response can be extended to the top of the target reservoir and possibly, to the surface or the seabed. Assuming that the caprock is impermeable and the largest pore pressure buildup is expected at the caprock-reservoir interface, the shear failure is possible at the interface. Once it is propagated to the caprock, its stability can be quite damaged. When there is a fault, it is exposed to the potential reactivation during the CO_2 injection process. The caprock can contain the fault or the failure from the fault can propagate to the caprock. In either case, the caprock stability is not secured. Once the caprock stability is not secured, buoyancy-driven leakage of the injected CO_2 is possible, which must be prevented for the environmental threat.

Since the density of injected CO_2 is lower than the formation water and it is floated upward to the interface of the caprock-reservoir, the weakest portion for the potential failure is the caprock-reservoir interface. Caprock failure may be the most concerned phenomenon during a CCS project, as it creates a pathway for CO_2 leakage to the surface or to a drinking water layer.

In addition, the CO_2 injection into underground geological structures may cause pore pressure buildup, and if severe, it can induce the pre-existing fault reactivation. When the faults are reactivated, they can be act as a path for CO_2 and induce micro-seismicity or even earthquakes which can be noticeable by the public. The Mohr-Coulomb failure criterion could be confirmed the value that fault may reactivate so we can evaluate stability of pre-existing faults. Because of this reason, several studies use the Mohr-Coulomb failure criterion to predict fault reactivation [13,14].

The innate pore volume of the underground geological structures is absolute, and the control of the pore pressure is key in determining the safe injection scheme of CCS project. When the pore pressure is increased, the poroelastic response of the rock may result in the deformation of the formation where severe amounts of CO_2 are injected. If the geomechanical properties of the overlying layers are considered, the CO_2 injection derived surface uplift can be calculated [15]. The uplift of the surface may lead to surface or seabed facility damages and threat the injection performance of the CCS projects [8,16].

Potential well integrity loss is also a major concern as the injected CO_2 can leak through the damaged cement or the space between the cement sheath and casing. The leaked fluid can contaminate the drinking groundwater [17]. One of the primary mechanisms is the casing or cement corrosion by the injected CO_2. The integrity of the casings and cements, used to protect hydrocarbon production/fluid injection wells from the reservoir conditions, can be lost by mechanical or chemical mechanisms after a long-term exposure to the CO_2 [18,19].

In summary, geomechanical risks can occur throughout the entire life of CCS projects. When the CO_2 is injected into the formation, a sharp increase in the pore pressure is expected because of the relatively low permeability of CO_2 when displacing the high viscous brine in the flow paths [20]. This may lead to the caprock instability and cause failure at the beginning of the injection. Continuous CO_2 injection causes gradual pore pressure increases around the near wellbore region. If the injection period is extended, the pore pressure may reach the fault reactivation pressure and induce the pre-existing fault slip [21]. In addition, the poroelastic response of the rock caused by the pore pressure buildup may result in the formation deformation such as the surface uplift. Meanwhile, the well integrity must be monitored during the entire CCS process, as the well is the primary flow path of the injected CO_2. The well integrity loss is more likely to occur when the casing or cement is damaged by the reaction with the injected CO_2. As the pore pressure increases, the damaged well components might not be able to sustain the external stress and to prevent the potential well collapse [22,23]. Each of these geomechanical risks can cause the injected CO_2 leakage, induced seismicity, surface uplift and the contamination of the drinking water-bearing-formation. Therefore, the geomechanical risks have to be taken into account for the optimal CCS project design.

3. Rock failure

Not only does the pressure change due to the injected fluid redistributes the stress state, but it also deteriorates the rock stability. Especially, since a caprock is an impermeable formation that isolates the target formation, its stability takes a major role in securing the geological structure by preventing leakage of the injected CO_2. The most vulnerable portion for the shear failure during the CO_2 injection is the interface of the caprock-reservoir where the largest pore pressure buildup is expected. If there is an existing fault in the target reservoir, it can be reactivated once the friction at the fault plane is reduced by the pore pressure. When the failure is occurred, the failure plane can be propagated to the caprock, which may induce the CO_2 leakage [24]. To avoid the undesirable consequence, the geomechanical analysis needs to be performed to identify the potential instability of the caprock when the CCS project is designed. In this section, the rock effective stress principle and possible failure types are addressed with the Mohr-Coulomb failure criterion for the caprock failure and fault reactivation analysis. Recent research trends on caprock failure and fault reactivation during CCS processes are also reviewed.

3.1. Effective stress principle of the rock

Rock is a type of porous medium, consisting of a rigid skeleton, interconnected pores, and fluids stored in the pores. The pore pressure is the pressure transmitted by the fluid in the rock, and the effective stress is the stress transferred by the interface between rock-solid particles. Upon CO_2 injection, inevitable pore pressure buildup decrease the effective stress in the affected region, which may destabilize the rock, cause failure of the structure and reactivate the neighboring faults [25]. The degree of effective stress change depends on the CO_2 injection rate and on the characteristics of the reservoir such as its permeability, porosity, and rock compressibility. Consequently, the pore pressure of the reservoir should be monitored during the entire CCS process to avoid any geomechanical risks. A number of laboratory experiments have presented that the pore pressure P has different effects on the failure of fully or partially saturated porous solid [26,27]. Terzaghi [28] proposed the effective stress principle to explain the mechanical response of porous media. In this study, the stress direction of tensile stress is

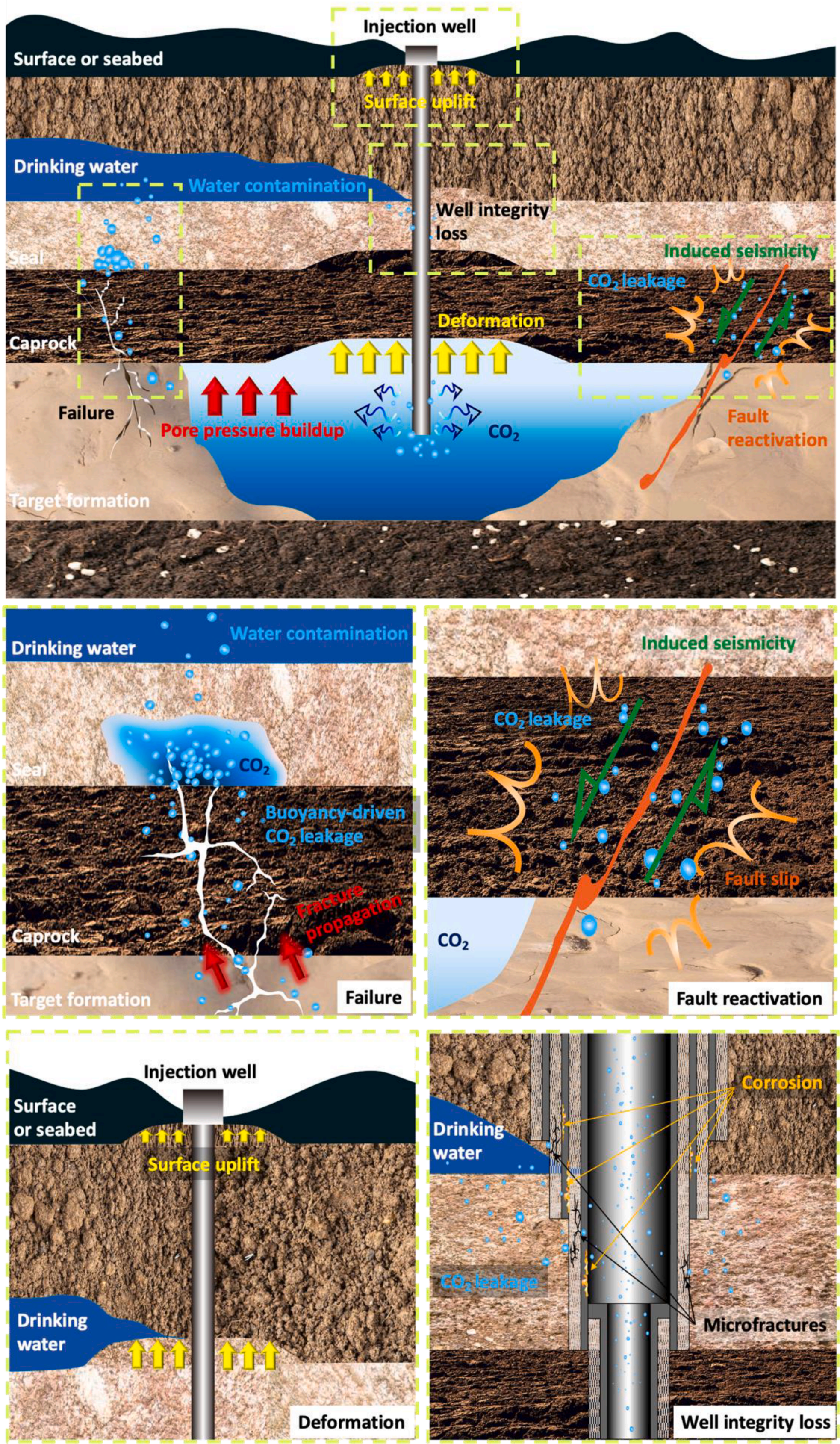

Fig. 1. Mechanisms of the potential geomechanical risks during CCS process.

defined as negative, and the pore pressure of the compressive stress is positive, which can be defined as follows [29]:

$$\sigma_{ij}^{'} = \sigma_{ij} + \alpha\delta_{ij}\left[\chi P_w + (1-\chi)P_g\right] \tag{1}$$

where $\sigma_{ij}^{'}$ is the effective stress, σ_{ij} is the total stress, δ_{ij} is Kronecker's delta, P_w and P_g are pore pressure of water and gas, respectively. χ is a coefficient related to the fluid saturation and surface tension. It is assumed that the pore is only filled by water and gas, i.e. $S_w + S_g = 1$. α is the Biot's coefficient, which is defined as,

$$\alpha = 1 - \frac{K_V}{K_S} \tag{2}$$

where K_V is the volumetric compression modulus of the rock and K_S is the compression modulus of solid particles. According to the Terzaghi's effective stress law, α is assumed to be 1.0 for the failure analysis. This is because the effect of the pore structure of rock is negligible when the rock is subject to failure [30]. Then, the effective stress can be expressed as,

$$\sigma_{ij}^{'} = \sigma_{ij} + \delta_{ij}[S_w P_w + (1-S_w)P_a] = \sigma_{ij} + \delta_{ij}\overline{P} \tag{3}$$

where $\overline{P}$ is the average pressure of the two fluids.

Related studies have shown that the CO_2 injection leads to an increase in the pore pressure, which deteriorates the rock [31–33]. When the stress redistributed by the pore pressure buildup meets the stress state that can induce the rock failure, the potential CO_2 flow through the generated failure planes may occur. If it flows further upward, the CO_2 can contaminate the aquifer and leak to the surface or seabed. Therefore, the stress distribution and the possibility of the caprock failure should be identified for a safe CCS process.

3.2. Failure criteria

There are three types of rock failure, compaction, tensile, and shear failure, as shown in Fig. 2.

Compaction failure occurs by pore collapse, and is less common during a CCS process because it requires high effective compressive stress to crush the pore space. Compaction failure may happen in nature due to rock burial, and also in the field of the petroleum engineering during reservoir depletion [15].

Tensile failure occurs when the effective stress is significantly reduced and below the tensile strength of rock. According to the theory of the strength of materials, the tensile failure criterion of caprock is defined as follows [34]:

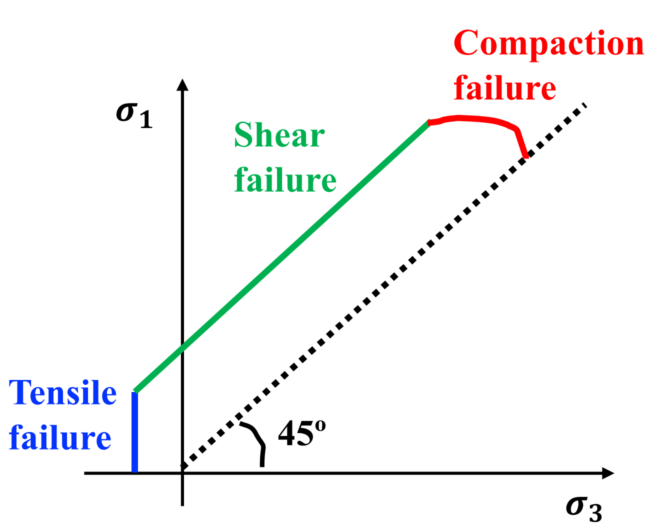

Fig. 2. Various failure types in principal stress space (modified [15]).

$$\sigma_3^{'} \leqslant \sigma_T \tag{4}$$

where $\sigma_3^{'}$ is the minimum principal effective stress and σ_T is the tensile strength. Comparing to the compressive strength of a rock, the tensile strength is relatively unimportant since rocks have low values. And when there is a discontinuity in a rock, it is generally assumed to be zero [35,36].

The most common type of failure is shear failure, which occurs when the shear stress acting on a caprock plane exceeds its shear strength at the fault plane. The Mohr-Coulomb criterion is the most widely used for identifying the shear failure of a rock. This is because it solely considers the maximum and minimum principal stresses, underestimate the rock strength and is therefore appropriate for the design purposes [37,38]. The shear stress τ is the stress component, which acts along the fracture plane as shown in Fig. 3. It is written using the principal stress components as follows:

$$|\tau| = c + \sigma_n^{'}\tan\phi \tag{5}$$

where τ is shear stress of shear plane, $\sigma_n^{'}$ is the effective normal stress, c is the cohesion of rock, and ϕ is the frictional angle of rock.

These effective normal stress and shear stress are obtained from the Mohr circle, which in equation form is [39]:

$$\sigma_n^{'} = \frac{(\sigma_1^{'} + \sigma_3^{'})}{2} + \frac{(\sigma_1 - \sigma_3)}{2}\cos 2\phi \tag{6}$$

$$\tau = -\frac{(\sigma_1 - \sigma_3)}{2}\sin 2\phi \tag{7}$$

where subscript 1 represents the maximum principal stress and subscript 3 represents the minimum principal stress. Shear failure can be represented graphically as the intersection of the Mohr circle with the Coulomb criterion as shown in Fig. 4.

There are two primary shear failure mechanisms during geological CO_2 storage are intact rock shear failure and fault reactivation. The pore

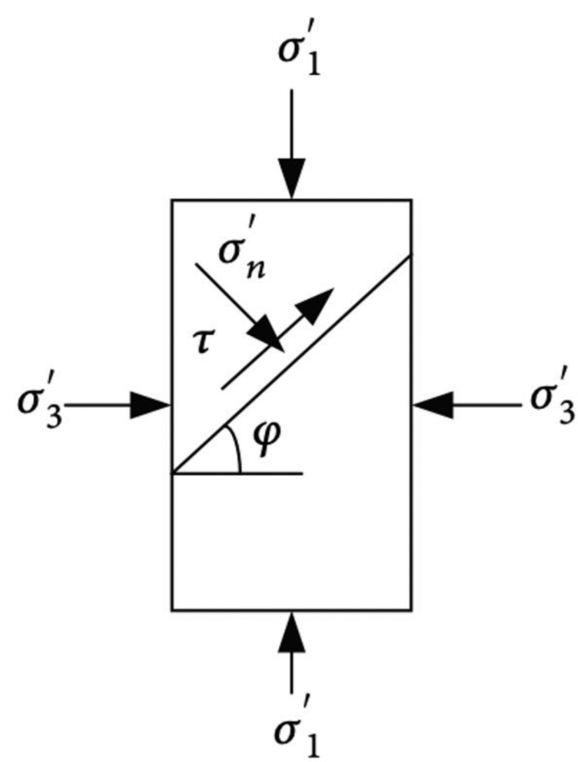

Fig. 3. Shear failure diagram.

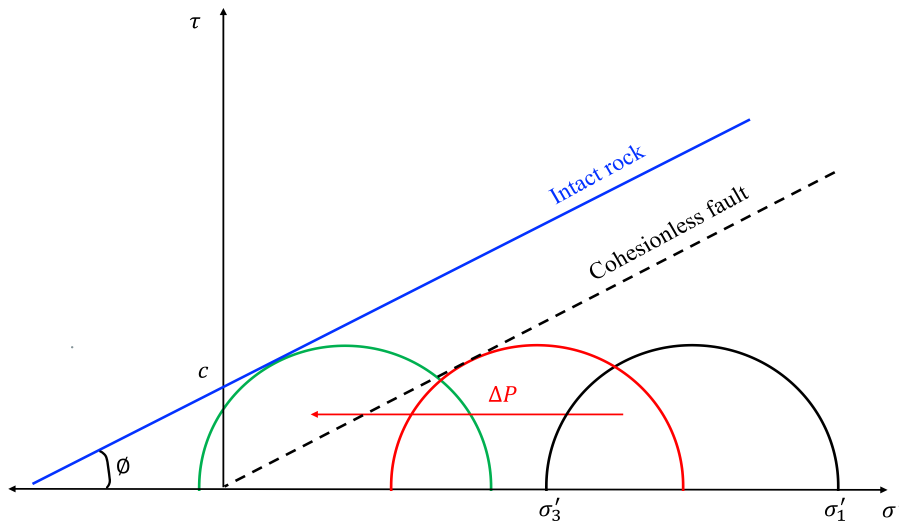

Fig. 4. Mohr circles with the Coulomb criteria showing failure envelopes. The blue line and black dashed line represent the failure envelopes of the intact rock and the cohesionless fault, respectively. Three stress states are shown, representing the stable state (black circle), shear failure on a cohesionless fault (red circle) and shear failure in an intact rock (green circle). If the pore pressure P increases due to the CO_2 injection, the circle moves to the left and reaches the failure envelope.

pressure buildup needed to trigger both failure mechanisms is evaluated with the Mohr-Coulomb failure criteria (Fig. 4). However, the onset of the two failure mechanisms take place at different conditions because the cohesion is neglected for the fault slip. If properties of the failure plane such as cohesion and friction angle are constant, the failure of a intact rock should occur after the reactivation of the fault due to the innate pure shear strength of the rock [40]. As shown in Fig. 4, black dashed line and blue line represent the failure envelope of a cohesionless fault and an intact rock, respectively. There are three stress states representing stable (black circle), shear failure on cohesionless fault (red circle) and shear failure in an intact rock (green circle). As the pore pressure buildup is induced during CO_2 injection, the Mohr circle moves to the left, approaching the failure envelope as the effective stress decreases. When the Mohr circle reaches the failure envelope of the cohesionless fault, the shear failure on the fault plane will occur. When there is no existing fault, the shear failure occurs at a higher pore pressure. Otherwise, if the Mohr circle constructed by the stress state does not meet the failure envelope, the rock is stable. Thus, if the effect of the pore pressure buildup is equally drawn in the same Mohr-Coulomb failure criteria, the Mohr circle would reach the failure envelope of the fault prior to the failure envelope of the intact rock.

3.3. *Caprock failure*

Upon the failure, the failure plane can propagate to the caprock and generate a flow path, which leads to unexpected CO_2 leakage to surface [41–43]. To investigate the possibility of the CO_2 leakage due to the caprock failure during a CCS project, several authors have conducted the numerical analysis for the potential failure of the caprock [44–47]. Dempsey et al. [44] analyzed mechanisms of the stress increment on the caprock failure. Higher stress increments are more likely to induce a fracture, to reactivate the critically stressed fault, and to threaten the caprock integrity. Moreover, they carried out the numerical simulation with the coupled thermos-hydro-mechanical code called the Finite Element for Heat and Mass Transfer (FEHM) to evaluate the caprock and fault stability. Therefore, prior to performing CCS, they proposed the potential range of the overpressured region should be analyzed through numerical modeling. Li et al. [45] performed the thermal-hydro-mechanical coupled simulations to investigate caprock failure under cooling and pressurization conditions during a CO_2 injection process. The authors presented the potential caprock failure increased with a higher value of the material parameter, R, which is defined as a ratio of the thermal expansion coefficient and the elastic properties of caprock and aquifer. They also presented that the consideration of the Biot's coefficient of the aquifer is essential for evaluating the potential caprock failure. Khan et al. [46] carried out the two-phase flow model simulation considering the Biyadh reservoir structure in Saudi Arabia to avoid CO_2 leakage due to the caprock failure. They considered both fractured and non-fractured caprocks to estimate safe parameter values during the CO_2 injection. For the non-fractured caprock, they concluded that the injected CO_2 is isolated within the caprock, while the CO_2 can leak through the fractured caprock, where the pore pressure rose as expected. Furthermore, they addressed that the closer the location of the fractured zone in the caprock to the injection well, the higher the pore pressure in the caprock. Xiao et al. [47] evaluated long-term caprock sealing capacity and effects of caprock hydrological and mineralogy heterogeneities on its integrity through coupled chemical–mechanical numerical simulation with geological model of the Farnsworth Unit (FWU). They founded out that Thirteen Fingers Limestone is an effective caprock that prevents supercritical CO_2 intrusion through capillary forces, and analyzed that the sealing efficiency of caprock improved by decreasing maximum porosity by up to 25 % due to mineral precipitation at the interface between caprock and reservoir. Therefore, they presented that the geomechanical response of caprocks due to CO_2 injection and mineral change has a low risk of induced fractures in the FWU.

In addition, several studies have analyzed the factors affecting the caprock failure during fluid injection [9,48]. Raziperchikolaee et al. [9] indicated that the variability of the in-situ stress affects the caprock and reservoir located in the Appalachian basin during the CO_2 injection. They also evaluated the fault reactivation, permeability enhancement, and CO_2 leakage. The authors constructed two coupled fluid flow-geomechanical models, i.e. a vertically heterogeneous but laterally homogeneous and a fully heterogeneous model, where a series of coupled fluid flow-reservoir geomechanics simulation were performed to investigate the impacts of in-situ stress variability, and evaluated the potential caprock failure with the estimated pressure and stress changes due to the CO_2 injection. By identifying the zones with potential caprock failure, they concluded that variation of the in-situ minimum horizontal stress is the most important factor when evaluating the geomechanical behavior during a CO_2 injection process in the Appalachian basin. Karimnezhad M. et al. [48] developed a three-dimensional (3D) finite element model with Abaqus and investigated the potential risk of the caprock failure during the CO_2 injection process, in terms of the pore pressure, vertical displacement of the caprock, and effective stress. It was found that the injection rate and initial stress state are the dominant factors in caprock failure. They also validated the results of the numerical model with analytical solutions.

3.4. Fault reactivation

A fault can function as a seal or a conductive channel that needs to be taken into account when a CCS process is designed. In a geomechanical point of view, faults can be reactivated which consequently leads to unexpected CO_2 leakage and undesirable seismicity [8]. Since the fault reactivation is a shear failure occurred at the fault, the Mohr-Coulomb failure criterion is also used for the fault reactivation analysis like caprock failure (Eq. (7)). The failure analysis of fault requires additional fault characteristics such as the inclination angle and shear strength of the fault plane, and the permeability of the fault. Thus, a more detailed Mohr-Coulomb failure analysis should be performed on faults compared to intact rocks [14]. Before injecting CO_2 into the formation, natural faults remain inactive under the persistent reservoir pressure. However, the unavoidable pore pressure buildup induced by the CO_2 injection may threaten the stability of faults. Because the effective normal stress acting on the fault plane is inversely proportional to the pore pressure, if the pore pressure change is significant, the shear stress acting on the fault plane may exceed the right-hand side of the Equation (7), and lead to fault slip [49]. During the CCS process, the CO_2 plume migrates out from the place of injection and the region affected by the reservoir pore pressure change is enlarged. If the plume reaches the pre-existing discontinuities such as fault and fracture zone, they experience effective normal stress decrease. When the stress drops under a specific level, the friction of the fault plane, the fault will destabilize and slip.

Many studies adopted numerical approaches to predict the fault slip during pore pressure buildup. Commercial simulators such as *GEM*, COMSOL, and ECLIPSE are widely used to model the reservoir geometry and to characterize the flow behaviors. The geomechanical properties are added with simulators like TOUGH, FLAC3D, and the geomechanical tools of CMG and PETREL to couple the flow behaviors with the geomechanical responses of the formation [25,33,43,50–55]. Zhao and Jha [55] developed and demonstrated a flow-geomechanical coupled modeling framework to evaluate the stability of the faults during CO_2 storage-enhanced oil recovery in the Farnsworth Unit (FWU) oil field in Texas, United States. Through this method, they founded out that the pressure buildup caused by water and CO_2 injection causes volumetric contraction and expansion of the reservoir and changes in the total and effective stresses in the overburden-reservoir-underburden structures. They also analyzed that these changes lead to alter in shear and effective normal stress for the three major faults in the FWU. Song and Wang [50] emphasized the risk of reactivating the adjacent faults of an CO_2 injection formation. For the purpose of mitigating the risk of reactivating the fault, artificial neural network (ANN) method was incorporated to determine the relief well location to maintain the pore pressure under the maximum allowable pressure. Khan et al. [25] related the effects of reservoir size and boundary conditions with fault slip. The simulation results showed that the relatively small sized reservoirs with closed boundary are opt to pressure buildup compared to bigger reservoirs. Thus, the results emphasized the importance of accurately modeling the reservoir size and boundary conditions in order to not under-estimate the pore pressure and cause fault slip. Rahman et al. [43] resampled the geomechanical properties inverted from seismic data to create a 3D grid of the reservoir and the overburden. The model could specify the overburden rock property with spatial variance and suggest a new failure mechanism for decision making.

The CO_2 injection rate and pore pressure should constantly be monitored at all stages of the CCS project especially when there is an adjacent fault. Rutqvist et al. [8] described procedures to determine the maximum sustainable injection pressure by a shear-slip analysis. A numerical analysis was also performed using TOUGH-FLAC, which determined the maximum sustainable CO_2 injection pressure.

There are studies focusing on the fluid transport properties of faults. The fault zone is divided into two structures, fault core and damaged zone, which have distinct permeability values. Cappa et al. [14] focused on the fault zone creation and its corresponding permeability heterogeneity. The authors were able to describe the mechanical deformation and fluid flow during the injection of CO_2 by analytically coupling the CO_2 flow rate and the permeability heterogeneity. In addition, Victor et al. [56] modeled a normal fault to simulate the pressure buildup near the low permeable faults during the CO_2 injection. They concluded that the permeability of the fault core is crucial for the fault stability because excessive overpressure can be induced by the impermeable interface. The fault plane heterogeneity was also studied by François et al. [31], who conducted lab-scale experiments to identify the effects of fluid injection rate on the pore pressure distribution over the fault planes. The results indicated that an updated nonlocal rupture initiation criterion should be appropriate for the higher injection rate as spatial pore pressure heterogeneity along the fault plane is expected. As shown in Fig. 5, the friction coefficient of the artificial fault is approximately 0.6, which was measured by the constant pore pressure along the fault plane (red stars in Fig. 5). It was found that the higher fluid injection rate generates significant pore pressure heterogeneity along the fault plane. As a result, the friction coefficient of the fault is larger at the moment of the fault slip (rectangles and circles in Fig. 5). Since the fault slip strongly depends on the injection rate of CO_2, it should be properly designed and constantly monitored during the CCS process.

In the prospective CO_2 storage site, Smeaheia, offshore Norway, Rahman et al. [57] investigated the hydromechanical effect on fault instability due to the injection-induced stress and pore pressure changes. Orlic [33] proceeded comparisons of the two main CO_2 injection sites, depleted Dutch gas fields and saline aquifers. Through numerical modeling and geomechanical analysis, it was concluded that more uncertainties remain in the characterizing of the aquifer whereas the depleted Dutch gas reservoir has more access to seismic data, logging data, and is proven with tight seal. Mustafa et al. [52] developed a two-way fully-coupled reservoir dynamic geomechanics model for the field M located at the north of Central Luconia Province in Sarawak Basin, Malaysia. CO_2 leakage from the reservoir due to fault reactivation and caprock integrity breach by the injection operation was evaluated. In North Sea, the numerical simulation of fracture generation and propagation caused by multiphase-flow was addressed by the cohesion zone

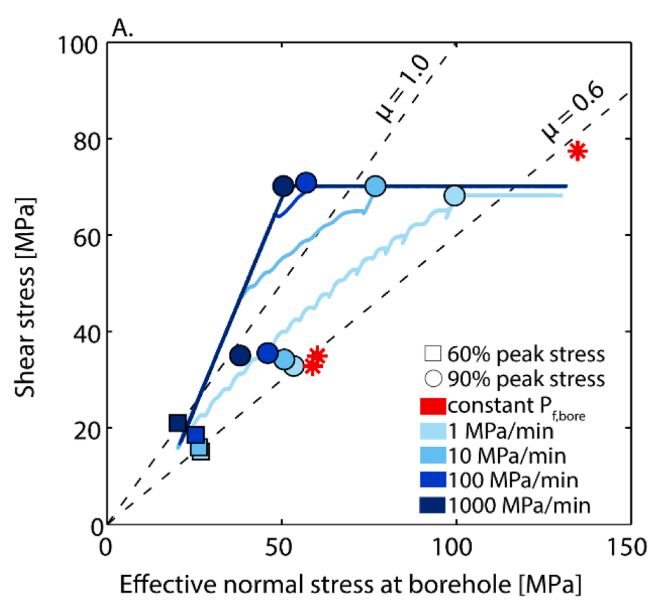

Fig. 5. Experimental results of static fault reactivation with different injection speeds [31]. (Square: onset of fault slip while the initial stress is 60% of the peak. Circle: onset of fault slip while the initial stress is 90% of the peak.)

modeling (CZM) [53].

4. Induced seismicity

Seismic activity is expected when the formation is failed with a newly created failure plane or with an existing fault reactivation. When the excessive pore pressure buildup is induced during a CCS process, the rock failure or the fault reactivation can occur with the subsequent seismic activity. If severe, the magnitude of the induced seismicity can be significant and may be perceivable by human sense. Noticeable induced seismicity not only threats the environment, but it also harms the public acceptance of the CCS project. Therefore, it is crucial to manage and to avoid it to achieve a successful implementation of CCS projects [58,59]. One of the most renowned examples of the induced seismicity by fluid injection into the ground occurred in Oklahoma in 2011 and 2012. The seismic activities with the magnitude of 5.6 were induced by the injection process at disposal wells in Oklahoma, which destroyed 14 buildings and injured two people [54]. Keranen et al. [60] analyzed the relationship between the wastewater injection and the induced earthquake events in Oklahoma in 2011 and 2012. It was found that a large time gap between the start of the injection and the actual earthquake occurrence is possible. Moreover, they pointed out that the volume injected into the underground should be adjusted to avoid reaching the critical reservoir pressure that might trigger slip of the adjacent faults. Weingarten et al. [61] examined the relationship between the induced seismicity and injection well types in the central and eastern United States (CEUS). They identified the tendency of the induced seismicity in wells injecting fluids for the enhanced oil recovery (EOR) method and salt water disposal (SWD) method. It was found that the number of the induced seismicity activities was higher in the SWD wells than in the EOR wells. Analyzing the SWD operations over states, they concluded that the higher the maximum injection rate, the higher the induced seismicity activities. However, in order to fully understand the potential of the induced seismicity, they suggested that a range of geologic, hydrogeologic, and operational conditions in the injection wells, which are potentially associated with the induced seismicity, should be analyzed.

In an attempt to create a model that distinguishes the seismic event source and the propagation methodology, Verdon et al. [62] developed a geomechanical model based on the micro-seismic activities of the Weyburn CO_2 storage site. The developed model allows to depict changes of the pore pressure and fracture potential of the target reservoir to determine the possibility of the injection-induced seismicity.

Since the subsequent induced seismicity is caused when the reservoir pore pressure exceeds the maximum allowable pressure, it is essential to manage the pressure by controlling the injection rate during the design stage of the CCS process. Zoback [63] emphasized that the induced seismicity due to fluid injection is a public concern and presented ways to effectively reduce the potential risks. The author proposed that minimizing the pore pressure buildup is clearly a good idea to reduce the potential of the injection-induced seismicity. The author also suggested that the operators and regulators should jointly establish operating protocols in areas where the potential injection-induced seismicity is a concern. These protocols are commonly referred as the traffic-light system. The traffic-light system restricts the injection rate upon a specific level of the induced seismicity. If the activity is severe, the system further terminates the injection process. Sites in Basel, Switzerland and Ohio, United States have adopted the traffic-light system to reduce the induced seismicity occurrences [64,65]. Yeo et al. [66] emphasized necessity of developing a casual mechanism for injection-induced earthquakes. They investigated the 2017 Pohang Mw 5.5 earthquake to link the effect of pore pressure change to the occurrence of the seismic events. During a CCS project, both the CO_2 injection rate and pressure should be monitored and managed under a certain level of pressure to avoid potential seismic events. Alghannam and Juanes [67] reported a management strategy during underground injection processes. It was found the injection-induced earthquakes are more affected by the injection rate than the injection volume. The observation was analyzed with a poroelastic model based on the rate-and-state friction theory. It was concluded that the risk of the induced earthquake is higher triggering when the injection period is shorter with the predetermined total injection volume.

5. Reservoir deformation

When CO_2 is injected into underground geologic storage target such as depleted hydrocarbon reservoirs, saline aquifers, and underground caverns, inevitable pore pressure buildup, effective stress alteration and subsequent reservoir deformation are expected [2,3]. In addition, the deformation at the top of the reservoir may be transmitted to the surface or seabed. For a safe and secure CCS process, the expected surface uplift due to the injection of CO_2 must be taken into consideration because it may induce damage to the surface facilities and stir public concerns. The surface deformation can be directly measured by the widely used surface measurement methods, such as the interferometric synthetic aperture radar (InSAR) and tiltmeters. For an offshore reservoir, however, direct measurements of the seabed deformation are not applicable. Therefore, the surface uplift caused by the CO_2 injection should be evaluated when a CCS process is designed.

The reservoir deformation can analytically be quantified with a few geomechanical variables. Fjaer et al. [15] presented a solution estimating the reservoir deformation caused by the pore pressure change. The equation requires the Young's modulus (E), Poisson's ratio (ν), and Biot's poroelastic constant (a) as inputs to depict the elastic changes of the reservoir thickness (Δh) as follows [13],

$$\Delta h = \frac{h}{E}\frac{(1+\nu)(1-2\nu)}{1-\nu}a\Delta P_f \tag{8}$$

Jun et al. [68] analytically quantified the surface uplift by the pore pressure change during CCS processes using Eq. (8). The authors incorporated the Gaussian pressure transient (GPT) method to determine the pore pressure distribution change by CO_2 injection, and the subsequent uplift was quantified. The results were validated with the InSAR measured uplift at the In Salah CO_2 storage project. Further application of the developed model was performed to estimate the seabed deformation and to evaluate the effect of the relief well on the mitigation of the uplift at the CCS candidate sites of South Korea, the Pohang basin and the depleted Donghae gas reservoir. The results in Fig. 6 show that up to 32 mm of uplift by the CCS process is expected at the seabed if CO_2 is injected into the reservoir for a year. However, the uplift can be mitigated by 17 mm if a water production well is operated nearby. The concept of the study emphasizes the importance of surface uplift calculation and suggests possible mitigation of the surface uplift.

On the other hand, there are many studies adopting numerical approaches to estimate the reservoir deformation with combining the reservoir flow simulator and the geomechanical models [27,46,69,70]. Examples of frequently used coupled simulators are TOUGH2-FLAC3D and COMSOL-GEM. [71], while ECLISPE-VISAGE and GEM-Geomechanical module are particularly powerful in modeling the geomechanical responses by CO_2 injection. Although the general governing equations of most simulators are based on the mass balance equation, the pressure responses brought by the CO_2 injection can show dissimilar results. ECLIPSE focuses on the reservoir management and monitoring throughout the entire project period. The constitutive relationship such as the Kozeny-Carman equation calculates the porosity, permeability and fluid saturations of the reservoir grid block and integrates a finite element model. The geomechanical module of GEM features the two-way coupling which enables the sequential calculation between the reservoir porosity and the time-dependent parameters such as the pore pressure and the principal stresses [72]. The capabilities and applications of different coupled simulators are presented in Table 1, which should be contemplated to model the geomechanical responses of CO_2

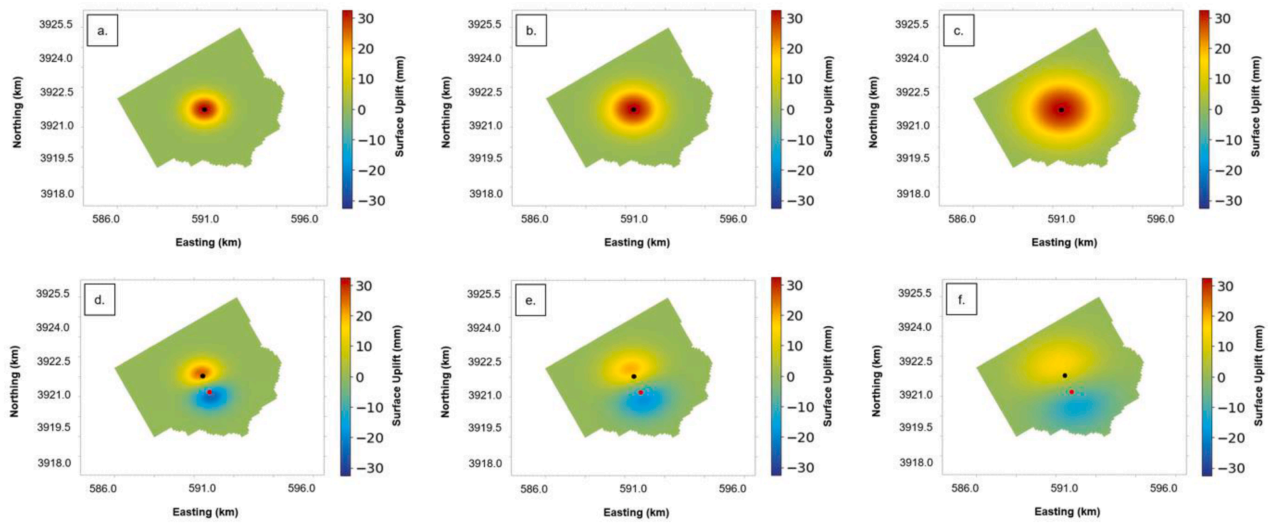

Fig. 6. Uplift calculated by the GPT-method in the Donghae gas reservoir: (a-c) 3, 6, and 12 months after injection without a relief well; (d-f) injection with a relief well, after 3, 6, and 12 months. Black and red dots represent the locations of the injection well and the relief well, respectively [68].

Table 1
Capabilities and applications of coupled simulators modeling geological CO_2 storage.

Simulator	Capacity	Application	Reference
GEM-COMSOL	• Multidimensional equation of state (EOS) simulator • Operation performed through custom script files • Single porosity and natural fracture modeling • Dual permeability modeling incorporating both matrix and fracture • Simultaneous modeling of production and injection processes • Geomechanical response after the production and injection	- CO_2 leakage Post-injection pore pressure distribution Surface uplift	Khan et al. [25,46]
Eclipse-VISAGE	• Two-way coupling of field-scale rock stress and strain response • Seismic resampling function distribute properties within the model grid • Sideburden, underburden and overburden plates populated into the grid • Calibration with lab measurement and wireline logs performed • Elastic and plastic deformation behavior governed by constitutive laws • Efficient pore pressure modeling with selected time-steps	- Ground deformation Vertical displacement at interface Rock failure	Rahman et al. [43], Mustafa et al. [52], Benisch et al. [72]
TOUGH-FLAC	• Coupled thermal–hydraulic–mechanical (THM) process modeling • Incorporates both continuum analysis and discrete fault analysis • Spatial evolution of stress field including site-specific geometry • Interfaces utilized to model the mechanical behavior of fault • Faults discretized considering mechanical and hydrologic properties	- Shear slip analysis Maximum sustainable CO_2 injection pressure Crustal deformation	Rutqvist et al. [8], Rinaldi et al, [69], Rutqvist [71]
ABAQUS	• Model transient and steady-state distribution of pore pressure • Consolidation modeling of fluid flow and deformation at low depth • Eight-node hexahedral displacement mesh modeling	- Injection induced pore pressure buildup Effective stress change	Karimnezhad et al. [48]
GEM-FLAC	• Explicit finite difference code • Initial stress change modeling due to injection induced pressure buildup	- Tensile and shear failure of caprock	Khazaei et al. [51]

injection accordingly.

A representative example of the surface uplift derived by a CCS project was observed in the In Salah CO_2 injection field of Algeria. Based on the satellite observed InSAR data, 15 to 22 mm of the surface has been uplifted by the injected CO_2 since 2004 [73]. Although the magnitude is only a few centimeters, the uplifted area has laterally extended up to 10 km. In addition, since it is accumulated with time, the effect should not be neglected if a long-term injection is planned.

To perform a coupling of fluid flow and geomechanical simulation, Rinaldi et al. [69] created a coupled model using TOUGH-FLAC. Fig. 7 shows the comparison between the InSAR observed line of sight (LOS) displacement for the KB-502 horizontal CO_2 injection well and the simulated LOS displacement of the same route. As the results indicate, the double-lobe uplift plum was matched with the observation and the surface uplift rates were simulated within 2 mm of deviation from the real data. The coupled modeling presented in Fig. 7 incorporates the well bottom hole pressure history, operation scheme, reservoir discontinuity characteristics, and the scaled spatial well locations of the CO_2 injection site. The development of the field-based model should be performed to preliminarily describe the surface uplift rates in the design phase of the project.

Another relevant study evaluated the effect of the CO_2 injection on the mitigation of the expected seabed subsidence by utilizing CO_2 enhanced gas recovery (EGR). The kinetic-reaction module of STARS

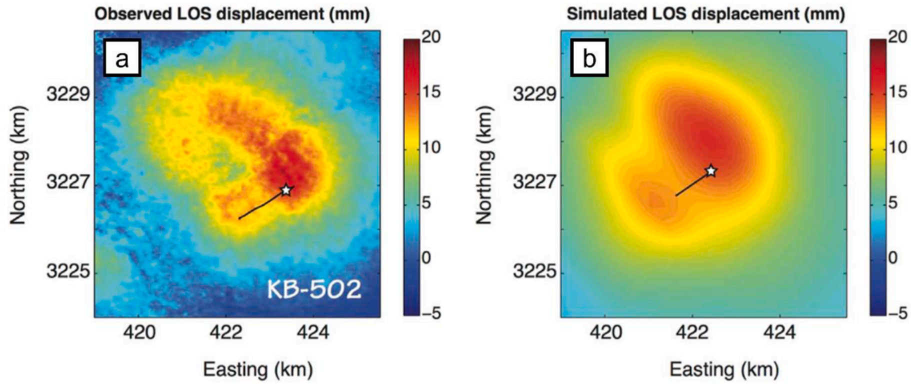

Fig. 7. (a) The observed line of sight (LOS) displacement for the KB-502 horizontal well. (b) The simulated LOS displacement of the identical region [69].

was adopted to model the depressurization and subsequent formation subsidence during the natural gas production. CO_2 injection into the corresponding formation was simulated and it was shown that the subsidence was significantly mitigated [74].

The relationship between the poroelastic response of the caprock and the surface uplift has been studied by Raziperchikolaee et al. [75]. They built a site-scale model of the depleted Michigan basin, calculated the stress changes, and determined the surface displacement. The outcomes were compared with the InSAR measurement. It was found that the presence of a low permeable caprock on top of the reservoirs helps diminish the uplift rates during the CCS project.

Injection well positioning is normally optimized by the maximum cumulative injection volume of CO_2, but it should further be corrected to minimize the geomechanical risks such as surface uplift, fault reactivation, and rock mechanical failure [50,70]. Khan et al. [76] examined the possibility of decreasing the pore pressure buildup by adopting a producing well next to the CO_2 injection well. The depleted Ghawar field was introduced as the CO_2 injection target and the CMG-GEM software was used for the reservoir flow simulation. It was concluded that the existence of the relief well aids the decrement of the pore pressure but the pressure depletion around the production well is still unavoidable.

6. Well integrity loss

Well integrity is defined as the application of technical, operational and organizational solutions to reduce the risk of uncontrolled release of formation fluids through the well components during the entire life cycle of the well [77]. When the well integrity is achieved for a well, the formation fluid will not be flowing through any component of the well except what was designed to be used as the flowing path. Therefore, loss of the well integrity implies that there would be formation fluid exchange between layers and potential upward fluid flow.

An injection well typically consists of at least two casings, which includes the surface casing cemented to the surface and the string casing that extends all the way to the injection zone. A tubing is located inside the long string casing from the ground surface to the injection zone [17]. During CCS process, CO_2 will pass the tubing and the perforations of the string casing, and flow into the target formation.

When CO_2 is injected and stored in a geologically secured structure, the injected CO_2 is completely isolated by the geological trap, such as a caprock and impermeable seals. Therefore, a well with penetrating the structure is the most vulnerable component that deteriorates the safe CO_2 storage. In other words, ensuring the well integrity is a key for successful CO_2 storage preventing potential CO_2 leakage to the surface or an adjacent permeable layer. For a depleted oil/gas reservoir, both the injection and abandoned wells are candidates for the CO_2 leakage [18]. In addition, when an old production well is repurposed for an injection well, ensuring the well integrity is an important process during the CCS design, as it will hold higher pressure than the outside of the well.

In the oil industry, poor well integrity causes various problems, including the formation fluid leakage to the surface, fluid migration between layers, and contamination of an aquifer. From a well integrity point of view, CO_2 is corrosive and chemically reacts with the casing and cement [78]. Mechanical degradation is also an important factor. As the pore pressure increases, the stress distribution near the wellbore alters. Combining with the mechanical degradations, the casing deformation and microcrack growth in the cement sheath may occur [79]. Since a well with damaged casing and cement is a highly conductive path for the potential CO_2 leakage, to secure the well integrity is essential during the CCS process [80]. The potential leakage pathways are shown in Fig. 8 [81].

This section introduced the fundamental mechanisms of the well integrity with casing and cementing.

6.1. Casing

Casing is used to isolate the wellbore from the formation and to support the wellbore from external stresses. In a long-term injection, wellbore components are constantly exposed to CO_2, and this may lead to corrosion. Especially for a depleted hydrocarbon reservoir, the existing well might not have been designed for the repurposed CO_2 injection and can be vulnerable to corrosion. Therefore, wells designed for CCS should consider the effect of the reaction between the casing and CO_2, as casing corrosion eventually results in well integrity loss. And the

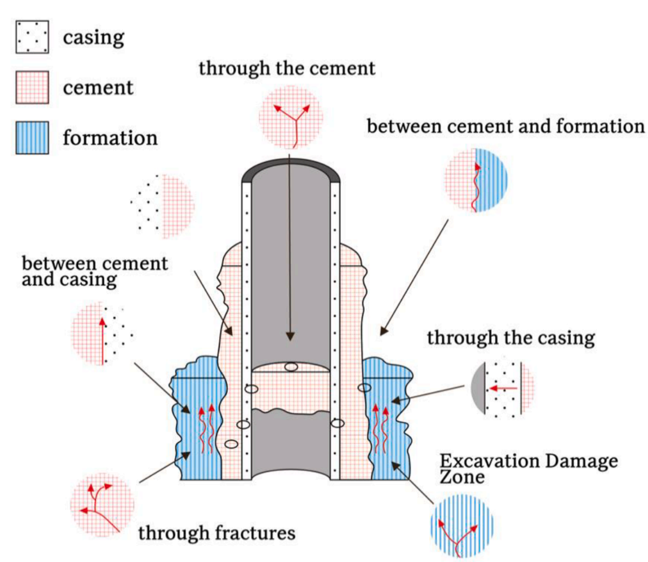

Fig. 8. Possible leakage pathways around the well [81].

casing can be deformed and its strength can be degraded. The reaction is an electrochemical corrosion, and the processes is as followed. First, the injected CO_2 reacts with the connate brine in the reservoir, making a carbonic acid.

$$CO_2(aq) + H_2O(l) \rightarrow H_2CO_3(aq) \tag{9}$$

And the reactions with the iron of the casing occur as the following steps,

$$Fe \rightarrow Fe^{2+} + 2e \tag{10}$$

$$Fe^{2+} + CO_3{}^{2-} \rightarrow FeCO_3 \tag{11}$$

$$Fe + 2HCO_3{}^{-} \rightarrow Fe(HCO_3)_2 \tag{12}$$

$$Fe(HCO_3)_2 \rightarrow FeCO_3 + CO_2 + H_2O \tag{13}$$

Which makes a corrosion product ($FeCO_3$) as a result shown in Equation (13). The rate of corrosion is decided by the temperature, pressure, salt concentration, pH, flow rate, and CO_2 partial pressure [82].

There are many studies related to casing corrosion caused by CO_2 [82–86]. Rida et al. [83] showed that the impact of salt concentration on the corrosion rate when exposed to both CO_2 and brine strongly depends on the CO_2 partial pressure. However, the results indicate that the temperature effect is negligible. At the low CO_2 partial pressure (P_{CO2}), the corrosion rate increases with the temperature up to 43 °C and declines above this temperature. Elgaddafi et al. [84] also conducted an experiment with 2 types of the API carbon steels, Q125 and T95, and concluded that the CO_2 corrosion rate of the API steels is sensitive to the fluid rate regardless of the temperature. In addition, it was found that the corrosion rate of the Q125 steel is more affected by the fluid flow than that of T95. Hoa et al. [85] used the carbon steel X70/1.8977, and suggested that care should be taken in choosing the cement type combined with high alloyed steel to avoid crevice corrosion and pitting in wellbore. Cul et al. [82] demonstrated that high NaCl concentrations increases the CO_2-NaCL corrosion at high temperature. In addition, the scanning electron microscope (SEM) results showed that the area of CO_2 corrosion became denser and uniform at high temperature. Lin et al. [86] developed a solution for the pipe based on the Von Mises yield criterion and the Lame thick-walled solution for the pipe. Combined with the experimental results, a modified casing design was proposed considering the effects of wear and corrosion on casing strength degradation.

On the other hand, Zeng et al. [87] demonstrated water-based annulus protection liquid for CO_2 injection wells. The corrosion inhibition rate of the water-based annulus protection liquid was higher than 98 % in the aqueous phase, and the corrosion rate of steel reached the corrosion control index of oil field (0.076 mm/s) in the gas-aqueous phase.

6.2. Cementing

Casings are cemented upon completion with the formation. In the oil industry, cement is mainly used for two purposes. Cement forms a sheath between the casing and the formation, to support and protect the casing by filling the space between the formation and the casing, and between the casings. Cement is also used for well abandonment, as cement plugs are placed inside the casing to isolate the reservoir to prevent liquid migration to other areas. In CCS, cement can be chemically reacted with the injected CO_2, resulting in the cement degradation and undesirable leakage.

First, the reaction of CO_2 and water, either co-injected or reservoir based, forms carbonic acid.

$$CO_2(aq) + H_2O(l) \rightarrow H_2CO_3(aq) \tag{14}$$

The acid contacts the cement in the well, causing carbonations.

$$Ca(OH)_2(s) + H_2CO_3(aq) \rightarrow CaCO_3(s) + 2H_2O(l) \tag{15}$$

And finally, the leaching out and precipitation of calcium carbonates occurs.

$$CaCO_3(s) + 2H_2O(l)^{-} \rightarrow Ca(OH)_2(s) + H_2CO_3(aq) \tag{16}$$

$$Ca(HCO_3)_2(s)^{-} \rightarrow 2CaCO_3(s) + H_2O(l) \tag{17}$$

The carbonation product ($Ca(OH)_2$) initially decreases the permeability and porosity. However, continuous exposure of CO_2 will increase the degree of carbonation. However, if $Ca(OH)_2$ becomes the dominant phase of the cement, strength degradation occurs, increasing the risk of potential fractures and cracks of the well cement [88]. Also, the degradation of cement will constantly weaken the casing, which would result in undesired leakage of CO_2. The rate of carbonation is affected by the pressure, temperature, and the gas concentration and the rate of degradation mainly depends on the cement quality and the cementing job quality [18].

There are several experimental studies of well integrity in CO_2 rich conditions [79,89–93]. Kutchko et al. [89] demonstrated that higher degree of hydration decreased the permeability, leading to increase of the cement's resistance to attack. Condor et al. [90] resulted in a decrease of permeability and an increase of compressive strength during the initial exposure of CO_2 in their experiment. The hydraulic and shear bonding also reduced after two months. The loss of strength was observed up to 65 % when CO_2 dissolved water was used in the experiment of Barlet-Gouedard et al. [91]. They also found that Portland cement is less affected in CO_2 exposure in brine. Omosebi et al. and Hwang et al. [92,93] concluded that temperature had a significant impact on the degree of carbonation than pressure and CO_2 composition. At constant temperatures, pressure was the main facture of the degradation of cement [88]. There are also different results, as Adeoye et al. [79] found that carbonation of Engineered Cementitious Composite (ECC) could lead to an increase in its compressive strength, and the damage was limited to microcracks in weeks of CO_2 disposure. Experiments held for cement degradation have various conditions, but they all conclude the degradation of cement must be considered in planning a CCS project.

Besides chemical reaction of casing and cement, mechanical issues are also known to affect well integrity. As pore pressure increases, there is a possibility of stress distribution alteration around the well, and this would lead to casing deformation or crack generation in the cementing [94]. Beside the increase of pore pressure, the cooling effect caused by the injected CO_2 can decrease the radial, axial and tangential stresses of the composite system, and these compressive stresses may turn to tensile stresses [95]. Possible failures caused by stress changes are shown in Fig. 9 [96]. Because of these reasons, considering chemical–mechanical combined effects is crucial for precise well integrity assessment [97]. Susan et al. [80] presented that chemical–mechanical effects have the potential to hinder the well integrity when a leakage path is already present due to cement shrinkage or fracturing, gaps along interfaces, or casing failures. Jung et al. [98] conducted an experiment in which CO_2-saturated groundwater and wet supercritical CO_2 reacted on fractures in cement/basalt samples to analyze the chemical–mechanical effects. They observed that carbonate precipitated from the fractures, causing the pressure changes, and isolating other cement fractures. They presented that the chemical effects have the potential to alter local stress in cement.

7. Discussion

During the geological CO_2 storage, the subsequent pore pressure increase may cause the geomechanical risks by the formation deformation and failure. The former is primarily caused by the poroelastic response of the rock, which result in the surface uplift. Although the surface uplift occurs with a low rate and is imperceptible, assessment of

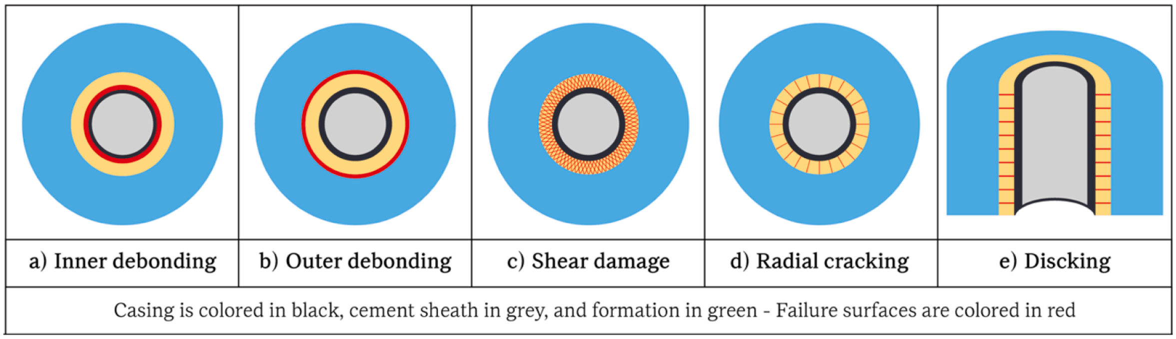

Fig. 9. Debonding of interfaces between casing-cement or cement sheath-rock, shear damage, radial cracking, and disking [96].

its timely cumulative effect should be monitored and managed as it occurs over a wide area. In addition, when an offshore field is targeted for the CO_2 storage, the uplift that may have a negative influence on the seabed ecosystem is difficult to monitor. Therefore, the potential surface or seabed uplift needs to be assessed and managed when the geological CO_2 storage is designed. If the stress magnitudes changed during the CO_2 injection exceeds the rock strength, the rock fails. In the same manner, when the pore pressure in the existing fault exceeds the maximum sustainable pressure, the fault slip may occur as the friction at the fault plane is insufficient to maintain the fault stability. Since the formation failure or the fault slip can generate new flow paths to outside of the secured geological structure, the phenomena need to be closely investigated to prevent the potential CO_2 leakage, which can lead to severe environmental hazards. Moreover, the induced seismicity needs to be avoided as it negatively affects the public acceptance on a CCS project. On the other hand, a loss of the well integrity can be aggravated by the CCS project with both chemical and mechanical mechanisms. The risk is more important when the CCS project is planned for a depleted hydrocarbon reservoir where a lot of wells exist.

Therefore, the potential geomechanical risks are closely related to the pore pressure buildup during the CO_2 injection. To prevent the formation failure and the fault slip, the pore pressure increment needs to be restricted not to damage the safe and secure the geological CO_2 storage site. For a hydrocarbon production, the high reservoir pressure is favorable as the fluid production can be facilitated with the lowering the bottomhole pressure (Fig. 10). When the bottomhole pressure is zero, it is called 'absolute open flow (AOF)', which means that the maximum fluid flow is made by the natural power of the reservoir. For a geological CO_2 storage, the injection pressure is restricted by the maximum allowable pressure of the reservoir, which is the maximum fluid pressure that does not induce the formation failure and fault reactivation. Therefore, determination of the safe injection pressure by the geomechanical analysis is closely related to the CO_2 storage capacity.

To maximize the storage capacity of the reservoir, there are several solutions. For example, controlling the operating conditions by monitoring the pore pressure buildup due to the CO_2 injection is an obviously effective option to improve the storage capacity. There is the permanent downhole gauge (PDG) method to monitor the pore pressure at the CO_2 injection site. PDG is a pressure (and/or temperature) gauge permanently installed in an oil/gas or injection well and can measure the tubing pressure and the annulus pressure [99–101]. PDG allows the well to be efficiently managed and optimized for operating conditions over the lifetime of the well. It is ideal to install multiple PDGs at different depths and as close to the target reservoir as possible. In addition, a well stimulation method can be applicable to enhance the permeability of the near-wellbore region and to improve the well injectivity. Moreover, operating a relief well can be another solution. Although drilling a new well or re-purposing an existing well requires additional cost, reducing the reservoir pressure can increase the CO_2 storage capacity. There are many studies focusing on operating the relief wells in terms of the operating condition, its locations and economic analysis [50,102–107]. The method would improve the storage capacity of aquifers by removing the formation fluid. Therefore, it can be a great solution for countries that do not have enough geological alternatives. However, it also should be noted that optimizing its location and operation conditions is crucial, as breakthrough of the injected CO_2 can occur and the operation would be stopped unexpectedly otherwise.

Furthermore, several studies have been carried out for the CO_2 injection through a horizontal well to improve the storage capacity with the lower pressure buildup [108–110]. This is because the increment of the pore pressure can be relieved if a horizontal well is used for the maximized injection intervals [109]. In addition, there are studies showing that injecting CO_2 through a vertical well causes a sharp pore pressure increase at the early stage of the process, because the relative permeability of CO_2 is quite restricted before the injected CO_2 establishes flow paths through the porous media as the viscosity of the displaced brine is much higher. After the pores in the vicinity of the injection well start to be filled with the injected CO_2, the relative permeability of CO_2 increases and the pore pressure slowly stabilizes. This phenomenon is defined as the pore pressure evolution, which has been observed in a field scale in the Ketsin pilot test site in Germany, in a semianalytical approach, and in numerical simulations [111–116]. Consequently, the geomechanical stability is more likely to improve with time when the vertical well injection is adopted. In contrast, the CO_2 injection at a constant mass flow rate through a horizontal well would result in the continuous pore pressure buildup and should be

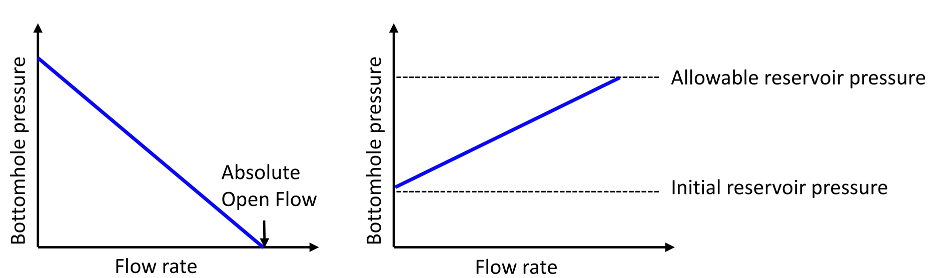

Fig. 10. The relationship between the bottomhole pressure and the flow rate. (a) For a hydrocarbon production field, the production flow rate increases as the bottomhole pressure reduces. (b) For a CCS project, the maximum injection pressure is restricted by the maximum allowable reservoir pressure.

avoided because the relative permeability of CO_2 is maintained low. There are studies that show that the continuous pore pressure buildup may cause rock failure after several years of injection from a horizontal well [21,115]. Moreover, Vilarrasa [20] indicated that the CO_2 injection through a vertical well is geomechanically more favorable than that of a horizontal well for several decades of the injection period. However, it was concluded that the stress field alteration due to the pore pressure changes should be taken into account to achieve more reliable results for each type of an injection well.

Recently, a lot of research activities about the CO_2 injection in an unconventional reservoir have been conducted to improve shale oil recovery accompanied with the CO_2 emission reduction [117–120]. CO_2 is an effective gas for enhanced oil recovery for unconventional reservoirs, as it is relatively easily miscible with oil, induces the oil swelling, and reduces the oil viscosity [121]. In addition, the CO_2 storage in unconventional reservoirs has a great potential due to the nanoporous structure that significantly increases the adsorption capacity. Thus, utilizing CO_2 to enhance the recovery of shale reservoirs and coalbed methane reservoirs recently gains researchers' interests [122]. Relevant researches have been conducted through molecular simulations, reservoir simulations, laboratory experiments, and field tests to demonstrate the potential of CO_2 utilization for CCS and enhanced oil/gas recovery in shale reservoirs [123–126]. For the CO_2 injection into the unconventional reservoir, geomechanical risks, such as rock failure, deformation, and well integrity loss presented in this study need to be integrated and investigated with effects of the adsorption, which will be performed in future studies.

8. Conclusion

In this paper, we reviewed mechanisms and related research activities of the potential geomechanical risks, i.e. CO_2 leakage, induced seismicity, surface uplift, and loss of the well integrity during the CCS. The major findings are as follows,

1. The formation can fail when the stress magnitudes exceed the strength of the rock. If the pore pressure at the existing fault exceeds the maximum sustainable pressure, the fault reactivation can occur. Since the formation failure and the fault reactivation can generate the new flow paths extended to outside of the secured geological structure, the injected CO_2 leakage may occur and the environmental hazard can be caused. In addition, these phenomena may cause the induced seismicity. When the magnitude of the induced seismicity is significant, it could threats the environments and distracts the public acceptance of the CCS project.
2. The CO_2 injection process induces unavoidable pore pressure buildup and effective stress alteration. These are causes of the subsequent reservoir deformation, and it can cause the deformation at the top of the reservoir transmitted to the surface or seabed. Due to this, reservoir deformation due to the CO_2 injection should be taken into consideration as it can damage the surface facilities and stir public concerns. For an offshore reservoir, direct measurements of the seabed deformation are not possible while there is a direct measurement method for onshore reservoir, such as the interferometric synthetic aperture radar (InSAR) and tiltmeters. Thus, the reservoir deformation due to the injection of CO_2 have to be evaluated, especially, when a CCS process is designed in offshore reservoir.
3. When the well integrity is lost, the formation fluid can leak through the elements of the well components and if severe, the injected CO_2 can be leaked to the surface and drinking water. These phenomena pose an environmental threat as they result in leakage to the atmosphere and contamination of the drinking water. Thus, the well integrity must be evaluated to prevent potential environmental threats. In particular, when an old production well is repurposed for an injection well, ensuring the well integrity should be taken into consideration during the CCS process design, as it will hold higher pressure than the outside of the well.

Therefore, the geomechanical analysis during the CCS process is of a critical importance for the environment and should be performed. Especially, concerns about the potential leakage of the injected CO_2, induced seismicity, surface uplift, and the contamination of the drinking water, are key geomechanical challenges that must be addressed when large-scale CCS processes are established.

Declaration of Competing Interest

The authors declare that they have no known competing financial interests or personal relationships that could have appeared to influence the work reported in this paper.

Data availability

Data will be made available on request.

Acknowledgement

This work is supported by Korea Agency for Infrastructure Technology Advancement grant funded by Ministry of Land, Infrastructure and Transport (22IFIP-C160208-06).

References

[1] Unfccc, Adoption of the paris agreement – Paris Agreement text English, 2015.
[2] S.M. Benson, D.R. Cole, CO2 sequestration in deep sedimentary formations, Elements. 4 (2008) 325–331.
[3] D. Zhu, S. Peng, S. Zhao, M. Wei, B. Bai, Comprehensive Review of Sealant Materials for Leakage Remediation Technology in Geological CO_2 Capture and Storage Process, (2021). doi: 10.1021/acs.energyfuels.0c04416.
[4] Energy Technology Perspectives 2020 - Special Report on Carbon Capture Utilisation and Storage, OECD, 2020. doi: 10.1787/208b66f4-en.
[5] G. of the R. of Korea, 2050 Carbon Neutral Strategy of the Republic of Korea: Towards a Sustainable and Green Society, (2020).
[6] Y. Song, C. Oh, Korea's Policy Direction on the Research & Development of Direct Air Carbon Capture and Storage (DACCS) Technologies: Focusing on DAC technologies, J. Clim. Chang. Res. 13 (2022) 75–96, https://doi.org/10.15531/ksccr.2022.13.1.075.
[7] J. Wang; R. Weijermars, Stress anisotropy changes near hydraulically fractured wells due to production-induced pressure-depletion, 2021.
[8] J. Rutqvist, J. Birkholzer, F. Cappa, C.F. Tsang, Estimating maximum sustainable injection pressure during geological sequestration of CO2 using coupled fluid flow and geomechanical fault-slip analysis, Energy Convers. Manage. 48 (2007) 1798–1807, https://doi.org/10.1016/J.ENCONMAN.2007.01.021.
[9] S. Raziperchikolaee, A. Pasumarti, The impact of the depth-dependence of in-situ stresses on the effectiveness of stacked caprock reservoir systems for CO2 storage, J. Nat. Gas Sci. Eng. 79 (2020), 103361, https://doi.org/10.1016/J.JNGSE.2020.103361.
[10] D. Li, S. Ren, H. Rui, CO2 Leakage Behaviors in Typical Caprock-Aquifer System during Geological Storage Process, ACS Omega. 4 (2019) 17874–17879, https://doi.org/10.1021/acsomega.9b02738.
[11] M.R. Amir Rashidi, E. Peter Dabbi, A.I. Azahree, Z.A. Abu Bakar, D. Tan Jen Huang, C. Pedersen, P. K. Tiwari, M.T. M Sallehud-Din, M.A. Shamsudin, M.K. Hamid, R. Tewari, P. A. Patil, CO2 Leakage Marine Dispersion Modelling for an Offshore Depleted Gas Field for CO2 Storage, in: Society of Petroleum Engineers (SPE), 2022. doi: 10.4043/31447-ms.
[12] J. Rutqvist, The geomechanics of CO2 storage in deep sedimentary formations, Geotech. Geol. Eng. 30 (2012) 525–551.
[13] S. Khan, Y. Khulief, A. Al-Shuhail, S. Bashmal, N. Iqbal, The geomechanical and fault activation modeling during co2 injection into deep minjur reservoir, eastern saudi arabia, Sustain. 12 (2020) 1–17, https://doi.org/10.3390/su12239800.
[14] F. Cappa, J. Rutqvist, Modeling of coupled deformation and permeability evolution during fault reactivation induced by deep underground injection of CO2, Int. J. Greenh. Gas Control. 5 (2011) 336–346, https://doi.org/10.1016/J.IJGGC.2010.08.005.
[15] R.M.H.P.H.A.M.R.& R.R. E. Fjaer, Petroleum Related Rock Mechanics 2nd Edition, 2008.
[16] X. Li, W. Yuan, B. Bai, M. Liu, H. He, Geomechanical Modeling of CO2 Storage in Deep Saline Aquifers – a Review, in: ISRM Int. Symp. - EUROCK 2013, 2013.
[17] K. Mortezaei, A. Amirlatifi, E. Ghazanfari, F. Vahedifard, Potential CO2leakage from geological storage sites: Advances and challenges, Environ. Geotech. 8 (2017) 3–27, https://doi.org/10.1680/jenge.18.00041.

[18] C. Teodoriu, O. Bello, A review of cement testing apparatus and methods under CO2 environment and their impact on well integrity prediction – Where do we stand? J. Pet. Sci. Eng. 187 (2020), 106736 https://doi.org/10.1016/J.PETROL.2019.106736.

[19] C.-F. Tsang, J. Birkholzer, J. Rutqvist, A comparative review of hydrologic issues involved in geologic storage of CO2 and injection disposal of liquid waste, Environ. Geol. 54 (2008) 1723–1737, https://doi.org/10.1007/s00254-007-0949-6.

[20] V. Vilarrasa, Impact of CO2 injection through horizontal and vertical wells on the caprock mechanical stability, Int. J. Rock Mech. Min. Sci. 66 (2014) 151–159, https://doi.org/10.1016/j.ijrmms.2014.01.001.

[21] J. Rutqvist, C.-F. Tsang, A study of caprock hydromechanical changes associated with CO2-injection into a brine formation, Environ. Geol. 42 (2002) 296–305, https://doi.org/10.1007/s00254-001-0499-2.

[22] K. Ravi, M. Bosma, L. Hunter, Optimizing the Cement Sheath Design in HPHT Shearwater Field, in: SPE/IADC Drill. Conf., OnePetro, 2003.

[23] J. Shaughnessy, J. Helweg, Optimizing HTHP cementing operations, IADC/SPE Drill. Conf., OnePetro (2002).

[24] V. Vilarrasa, R.Y. Makhnenko, Caprock Integrity and Induced Seismicity from Laboratory and Numerical Experiments, Energy Procedia. 125 (2017) 494–503, https://doi.org/10.1016/J.EGYPRO.2017.08.172.

[25] S. Khan, Y.A. Khulief, · A A Al-Shuhail, A.A. Al-Shuhail, Effects of reservoir size and boundary conditions on pore-pressure buildup and fault reactivation during CO 2 injection in deep geological reservoirs, 79 (2020) 294. doi: 10.1007/s12665-020-09040-0.

[26] S. Raziperchikolaee, S. Mishra, Statistical based hydromechanical models to estimate poroelastic effects of CO2 injection into a closed reservoir, Greenh. Gases Sci. Technol. 10 (2020) 176–195, https://doi.org/10.1002/ghg.1956.

[27] H.J. Siriwardane, R.K. Gondle, S.B. Varre, G.S. Bromhal, T.H. Wilson, Geomechanical response of overburden caused by CO2 injection into a depleted oil reservoir, J. Rock Mech. Geotech. Eng. 8 (2016) 860–872, https://doi.org/10.1016/J.JRMGE.2016.06.009.

[28] K. Terzaghi, R.B. Peck, G. Mesri, Soil mechanics in engineering practice, John Wiley & Sons, 1996.

[29] X. Su, A. Mehrabian, Coupled poroelastic solutions for the reservoir and caprock layers with the overburden confinement effects, Geomech. Energy Environ. 25 (2021), 100215, https://doi.org/10.1016/J.GETE.2020.100215.

[30] M. Wangen, S. Gasda, T. Bjørnarå, Geomechanical Consequences of Large-scale Fluid Storage in the Utsira Formation in the North Sea, Energy Procedia. 97 (2016) 486–493, https://doi.org/10.1016/J.EGYPRO.2016.10.056.

[31] F.X. Passelègue, N. Brantut, T.M. Mitchell, Geophysical Research Letters Fault Reactivation by Fluid Injection: Controls from Stress State and Injection Rate, (2018). doi: 10.1029/2018GL080470.

[32] K. Kim, V. Vilarrasa, R.Y. Makhnenko, CO2 Injection Effect on Geomechanical and Flow Properties of Calcite-Rich Reservoirs, Fluids. 3 (2018), https://doi.org/10.3390/fluids3030066.

[33] B. Orlic, Geomechanical effects of CO2 storage in depleted gas reservoirs in the Netherlands: Inferences from feasibility studies and comparison with aquifer storage, J. Rock Mech. Geotech. Eng. 8 (2016) 846–859, https://doi.org/10.1016/j.jrmge.2016.07.003.

[34] A. Minardi, E. Stavropoulou, T. Kim, A. Ferrari, L. Laloui, Experimental assessment of the hydro-mechanical behaviour of a shale caprock during CO2 injection, Int. J. Greenh. Gas Control. 106 (2021), 103225, https://doi.org/10.1016/J.IJGGC.2020.103225.

[35] D.A. Lockner, Rock Failure, Rock Phys, Phase Relations. (1995) 127–147, https://doi.org/10.1029/RF003p0127.

[36] M.D. Zoback, Reservoir geomechanics, Cambridge University Press, 2010.

[37] undefined N. H. W., J. C. Jaeger & N. G. W. Cook 1979. Fundamentals of Rock Mechanics. 3rd edition. xix+593 pp., numerous figs. London: Chapman and Hall. ISBN 0 412 22010 5. Price £9.95., Geol. Mag. 117 (1980) 401. doi: DOI: 10.1017/S001675680003274X.

[38] J.F. Labuz, A. Zang, J.F. Labuz, A. Zang, Mohr-Coulomb Failure Criterion 45 (2012) 975–979, https://doi.org/10.1007/s00603-012-0281-7.

[39] J.C. Jaeger, N.G.W. Cook, R. Zimmerman, Fundamentals of rock mechanics, John Wiley & Sons, 2009.

[40] L. Chiaramonte, J.A. White, W. Trainor-Guitton, Probabilistic geomechanical analysis of compartmentalization at the Snøhvit CO 2 sequestration project, (2015). doi: 10.1002/2014JB011376.

[41] C.D. Hawkes, P.J. McLellan, U. Zimmer, S. Bachu, Geomechanical factors affecting geological storage of CO2 in depleted oil and gas reservoirs: risks and mechanisms, in: Gulf Rocks 2004, 6th North Am. Rock Mech. Symp., OnePetro, 2004.

[42] S.H. Hajiabadi, P. Bedrikovetsky, S. Borazjani, H. Mahani, Well Injectivity during CO2 Geosequestration: A Review of Hydro-Physical, Chemical, and Geomechanical Effects, Energy & Fuels. 35 (2021) 9240–9267, https://doi.org/10.1021/acs.energyfuels.1c00931.

[43] M.J. Rahman, M. Fawad, J. Chan Choi, N.H. Mondol, Effect of overburden spatial variability on field-scale geomechanical modeling of potential CO2 storage site Smeaheia, offshore Norway, J. Nat. Gas Sci. Eng. 99 (2022), https://doi.org/10.1016/j.jngse.2022.104453.

[44] D. Dempsey, S. Kelkar, R. Pawar, E. Keating, D. Coblentz, Modeling caprock bending stresses and their potential for induced seismicity during CO2 injection, Int. J. Greenh. Gas Control. 22 (2014) 223–236, https://doi.org/10.1016/j.ijggc.2014.01.005.

[45] C. Li, L. Laloui, Impact of material properties on caprock stability in CO2 geological storage, Geomech, Energy Environ. 11 (2017) 28–41, https://doi.org/10.1016/J.GETE.2017.06.003.

[46] S. Khan, Y.A. Khulief, A. Al-Shuhail, Mitigating climate change via CO 2 sequestration into Biyadh reservoir: geomechanical modeling and caprock integrity, (n.d.). doi: 10.1007/s11027-018-9792-1.

[47] T. Xiao, H. Xu, N. Moodie, R. Esser, W. Jia, L. Zheng, J. Rutqvist, B. McPherson, Chemical-Mechanical Impacts of CO2 Intrusion Into Heterogeneous Caprock, Water Resour. Res. 56 (2020) e2020WR027193. doi: doi: 10.1029/2020WR027193.

[48] M. Karimnezhad, H. Jalalifar, M. Kamari, Investigation of caprock integrity for CO2 sequestration in an oil reservoir using a numerical method, J. Nat. Gas Sci. Eng. 21 (2014) 1127–1137, https://doi.org/10.1016/j.jngse.2014.10.031.

[49] P. Pan, Z. Wu, X. Feng, F. Yan, Geomechanical modeling of CO2 geological storage: A review, J. Rock Mech. Geotech. Eng. 8 (2016) 936–947, https://doi.org/10.1016/J.JRMGE.2016.10.002.

[50] Y. Song, J. Wang, Optimization of Relief Well Design Using Artificial Neural Network during Geological CO 2 Storage in Pohang Basin, South Korea Optimization of Relief Well Design Using Artificial Neural Network during Geological CO 2 Storage in, (2021). doi: 10.3390/app11156996.

[51] C.K.R. Chalaturnyk, A Reservoir-Geomechanical Model to Study the Likelihood of Tensile and Shear Failure in the Caprock of Weyburn CCS Project with Regard to Interpretation of Microseismic Data, (n.d.). doi: 10.1007/s10706-017-0262-4.

[52] M.A. Mustafa, S.S.M. Ali, M.H. Yakup, C.P. Tan, Integrated 2-Way Fully Coupled Reservoir Dynamic-Geomechanical Modelling Approach for CO2 Storage Risk Assessment in a Malaysian Carbonate Field, Society of Petroleum Engineers (SPE) (2022), https://doi.org/10.2523/iptc-22685-ms.

[53] J. Park, L. Griffiths, J. Dautriat, L. Grande, I.V. Rodriguez, K. Iranpour, T. I. Bjørnarå, H.M. Moreno, N.H. Mondol, G. Sauvin, J. Sarout, M. Soldal, V. Oye, D. N. Dewhurst, J.C. Choi, A.I. Best, Induced-seismicity geomechanics for controlled CO2 storage in the North Sea (IGCCS), Int. J. Greenh. Gas Control. 115 (2022), https://doi.org/10.1016/j.ijggc.2022.103614.

[54] E.W. L., Injection-Induced Earthquakes, Science (80-). 341 (2013) 1225942. doi: 10.1126/science.1225942.

[55] X. Zhao, B. Jha, Role of Well Operations and Multiphase Geomechanics in Controlling Fault Stability During CO 2 Storage and Enhanced Oil Recovery, (2019). doi: 10.1029/2019JB017298.

[56] V. Vilarrasa, R. Makhnenko, S. Gheibi, Geomechanical analysis of the influence of CO2 injection location on fault stability, J. Rock Mech. Geotech. Eng. 8 (2016) 805–818, https://doi.org/10.1016/J.JRMGE.2016.06.006.

[57] J. Rahman, M. Fawad, N.H. Mondol, 3D Field-Scale Geomechanical Modeling of Potential CO 2 Storage Site Smeaheia, Offshore Norway (2022), https://doi.org/10.3390/en15041407.

[58] C. Technologies, C. Resources, C. Engineering, C. Geodynamics, B. Resources, D. Studies, N. Council, Induced seismicity potential in energy technologies, 2013. doi: 10.17226/13355.

[59] A. Paluszny, C.C. Graham, K.A. Daniels, V. Tsaparli, D. Xenias, S. Salimzadeh, L. Whitmarsh, J.F. Harrington, R.W. Zimmerman, Caprock integrity and public perception studies of carbon storage in depleted hydrocarbon reservoirs, Int. J. Greenh. Gas Control. 98 (2020), 103057, https://doi.org/10.1016/J.IJGGC.2020.103057.

[60] K.M. Keranen, H.M. Savage, G.A. Abers, E.S. Cochran, Potentially induced earthquakes in Oklahoma, USA: Links between wastewater injection and the 2011 Mw 5.7 earthquake sequence, Geology. 41 (2013) 699–702, https://doi.org/10.1130/G34045.1.

[61] M. Weingarten, S. Ge, J.W. Godt, B.A. Bekins, J.L. Rubinstein, High-rate injection is associated with the increase in U.S. mid-continent seismicity, Science (80-) 348 (2015) 1336–1340, https://doi.org/10.1126/science.aab1345.

[62] J.P. Verdon, J.M. Kendall, D.J. White, D.A. Angus, Linking microseismic event observations with geomechanical models to minimise the risks of storing CO2 in geological formations, Earth Planet. Sci. Lett. 305 (2011) 143–152, https://doi.org/10.1016/J.EPSL.2011.02.048.

[63] M.D. Zoback, Managing the seismic risk posed by wastewater disposal, Earth. 57 (2012) 38.

[64] N. Deichmann, D. Giardini, Earthquakes induced by the stimulation of an enhanced geothermal system below Basel (Switzerland), Seismol. Res. Lett. 80 (2009) 784–798.

[65] W. Kim, Induced seismicity associated with fluid injection into a deep well in Youngstown, Ohio, J. Geophys. Res. Solid Earth. 118 (2013) 3506–3518.

[66] I.W. Yeo, M.R. M Brown, S. Ge, K.K. Lee, Causal mechanism of injection-induced earthquakes through the M w 5.5 Pohang earthquake case study, (2020). doi: 10.1038/s41467-020-16408-0.

[67] M. Alghannam, R. Juanes, Understanding rate effects in injection-induced earthquakes, (2020). doi: 10.1038/s41467-020-16860-y.

[68] S. Jun, Y. Song, J. Wang, Formation Uplift Analysis During Geological CO 2-Storage Using the Gaussian Pressure Transient Method: Krechba (Algeria) Validation and South Korean Case Studies, J. Pet. Sci. Eng. (2022), https://doi.org/10.2139/ssrn.4170649 (under review).

[69] A.P. Rinaldi, J. Rutqvist, S. Finsterle, H.H. Liu, Inverse modeling of ground surface uplift and pressure with iTOUGH-PEST and TOUGH-FLAC: The case of CO2 injection at In Salah, Algeria, Comput. Geosci. 108 (2017) 98–109, https://doi.org/10.1016/J.CAGEO.2016.10.009.

[70] F. Zheng, A. Jahandideh, B. Jha, B. Jafarpour, Geologic CO2 Storage Optimization under Geomechanical Risk Using Coupled-Physics Models, Int. J. Greenh. Gas Control. 110 (2021), https://doi.org/10.1016/j.ijggc.2021.103385.

[71] J. Rutqvist, Status of the TOUGH-FLAC simulator and recent applications related to coupled fluid flow and crustal deformations, Comput. Geosci. 37 (2011) 739–750, https://doi.org/10.1016/j.cageo.2010.08.006.
[72] K. Benisch, B. Graupner, S. Bauer, The Coupled OpenGeoSys-eclipse Simulator for Simulation of CO2 Storage – code Comparison for Fluid Flow and Geomechanical Processes, Energy Procedia. 37 (2013) 3663–3671, https://doi.org/10.1016/J.EGYPRO.2013.06.260.
[73] B. Bohloli, T.I. Bjørnarå, J. Park, A. Rucci, Can we use surface uplift data for reservoir performance monitoring? A case study from In Salah, Algeria, Int. J. Greenh. Gas Control. 76 (2018) 200–207, https://doi.org/10.1016/J.IJGGC.2018.06.024.
[74] T.-K. Lin, B.-Z. Hsieh, Prevention of Seabed Subsidence of Class-1 Gas Hydrate Deposits via CO 2-EGR: A Numerical Study with Coupled Geomechanics-Hydrate Reaction-Multiphase Fluid Flow Model, (2020). doi: 10.3390/en13071579.
[75] S. Raziperchikolaee, Z. Cotter, N. Gupta, Assessing mechanical response of CO2 storage into a depleted carbonate reef using a site-scale geomechanical model calibrated with field tests and InSAR monitoring data, J. Nat. Gas Sci. Eng. 86 (2021), 103744, https://doi.org/10.1016/J.JNGSE.2020.103744.
[76] S. Khan, Y.A. Khulief, A A Al-Shuhail, Alleviation of pore pressure buildup and ground uplift during carbon dioxide injection into Ghawar Arab-D carbonate naturally fractured reservoir, 77 (2018) 449. doi: 10.1007/s12665-018-7610-4.
[77] Norsok Standard D-010 Well Integrity in Drilling and Well Operations, (n.d.).
[78] M. Bai, Z. Zhang, X. Fu, A review on well integrity issues for CO2 geological storage and enhanced gas recovery, Renew. Sustain. Energy Rev. 59 (2016) 920–926, https://doi.org/10.1016/J.RSER.2016.01.043.
[79] J.T. Adeoye, C. Beversluis, A. Murphy, V.C. Li, B.R. Ellis, Physical and chemical alterations in engineered cementitious composite under geologic CO2 storage conditions, Int. J. Greenh. Gas Control. 83 (2019) 282–292, https://doi.org/10.1016/J.IJGGC.2019.01.025.
[80] S. Carroll, J.W. Carey, D. Dzombak, N.J. Huerta, L. Li, T. Richard, W. Um, S.D. C. Walsh, L. Zhang, Review: Role of chemistry, mechanics, and transport on well integrity in CO2 storage environments, Int. J. Greenh. Gas Control. 49 (2016) 149–160, https://doi.org/10.1016/j.ijggc.2016.01.010.
[81] K.M. Reinicke, C. Fichter, Measurement strategies to evaluate the integrity of deep wells for CO2 applications, Undergr. Storage CO2, Energy. (2010) 67.
[82] L. Cui, W. Kang, H. You, · Jiarui Cheng, Z. Li, Experimental Study on Corrosion of J55 Casing Steel and N80 Tubing Steel in High Pressure and High Temperature Solution Containing CO 2 and NaCl, J. Bio- Tribo-Corrosion. 7 (2021) 13. doi: 10.1007/s40735-020-00449-5.
[83] R. Elgaddafi, R. Ahmed, S. Shah, Corrosion of carbon steel in CO2 saturated brine at elevated temperatures, J. Pet. Sci. Eng. 196 (2021), 107638, https://doi.org/10.1016/J.PETROL.2020.107638.
[84] R. Elgaddafi, R. Ahmed, S. Shah, The effect of fluid flow on CO2 corrosion of high-strength API carbon steels, J. Nat. Gas Sci. Eng. 86 (2021), 103739, https://doi.org/10.1016/J.JNGSE.2020.103739.
[85] L. Quynh Hoa, R. Bäßler, D. Bettge, E. Buggisch, B. Nicole Schiller, M. Beck, Corrosion Study on Wellbore Materials for the CO 2 Injection Process, (2021). doi: 10.3390/pr9010115.
[86] T. Lin, Q. Zhang, Z. Lian, X. Chang, K. Zhu, Y. Liu, Evaluation of casing integrity defects considering wear and corrosion – Application to casing design, J. Nat. Gas Sci. Eng. 29 (2016) 440–452, https://doi.org/10.1016/J.JNGSE.2016.01.029.
[87] D. Zeng, B. Dong, Z. Yu, Z. Huang, Y. Yi, H. Yu, J. Li, G. Tian, Design of water-based annulus protection fluid for CO2 flooding injection well, J. Pet. Sci. Eng. 205 (2021), 108726, https://doi.org/10.1016/J.PETROL.2021.108726.
[88] O. Omosebi, H. Maheshwari, R. Ahmed, S. Shah, S. Osisanya, S. Hassani, G. DeBruijn, W. Cornell, D. Simon, Degradation of well cement in HPHT acidic environment: Effects of CO2 concentration and pressure, Cem. Concr. Compos. 74 (2016) 54–70, https://doi.org/10.1016/J.CEMCONCOMP.2016.09.006.
[89] B.G. Kutchko, B.R. Strazisar, D.A. Dzombak, G.V. Lowry, N. Thauiow, Degradation of well cement by CO2 under geologic sequestration conditions, Environ. Sci. Technol. 41 (2007) 4787–4792, https://doi.org/10.1021/ES062828C.
[90] J. Condor, K. Asghari, Experimental Study of Stability and Integrity of Cement in Wellbores Used for CO2 Storage, Energy Procedia. 1 (2009) 3633–3640, https://doi.org/10.1016/J.EGYPRO.2009.02.159.
[91] V. Barlet-Gouédard, G. Rimmelé, O. Porcherie, N. Quisel, J. Desroches, A solution against well cement degradation under CO2 geological storage environment, Int. J. Greenh. Gas Control. 3 (2009) 206–216, https://doi.org/10.1016/J.IJGGC.2008.07.005.
[92] O. Omosebi, H. Maheshwari, R. Ahmed, S. Shah, S. Osisanya, A. Santra, A. Saasen, Investigating temperature effect on degradation of well cement in HPHT carbonic acid environment, J. Nat. Gas Sci. Eng. 26 (2015) 1344–1362, https://doi.org/10.1016/J.JNGSE.2015.08.018.
[93] J. Hwang, R. Ahmed, S. Tale, S. Shah, Shear bond strength of oil well cement in carbonic acid environment, J. CO2 Util. 27 (2018) 60–72, https://doi.org/10.1016/J.JCOU.2018.07.001.
[94] P.A. Patil, A.M. Hamimi, M.A.B. Abu Bakar, D.P. Das, P.K. Tiwari, P. Chidambaram, M.A. B. A. Jalil, Scrutinizing Wells Integrity for Determining Long-Term Fate of a CO2 Sequestration Project: An Improved and Rigorous Risk Assessment Strategy, in: Society of Petroleum Engineers (SPE), 2022. doi: 10.2523/iptc-22348-ms.
[95] M. Bai, J. Sun, K. Song, K.M. Reinicke, C. Teodoriu, Evaluation of mechanical well integrity during CO 2 underground storage, (n.d.). doi: 10.1007/s12665-015-4157-5.
[96] A.-P. Bois, ; A Garnier, G. Galdiolo, J.-B. Laudet, SPE 139668 Use of a Mechanistic Model To Forecast Cement-Sheath Integrity for CO 2 Storage, 2010. http://onepetro.org/SPECO2/proceedings-pdf/10CO2/All-10CO2/SPE-139668-MS/1756666/spe-139668-ms.pdf/1.
[97] Y. Feng, Geomechanics of Geological Carbon Sequestration, in: S.Z.E.-D.S.S.E.-D. K. Karthikeyan (Ed.), Carbon Sequestration, IntechOpen, Rijeka, 2022: p. Ch. 5. doi: 10.5772/intechopen.105412.
[98] H.B. Jung, W. Um, Experimental study of potential wellbore cement carbonation by various phases of carbon dioxide during geologic carbon sequestration, Appl. Geochem. 35 (2013) 161–172, https://doi.org/10.1016/j.apgeochem.2013.04.007.
[99] R.N. Horne, Listening to the reservoir—interpreting data from permanent downhole gauges, J. Pet. Technol. 59 (2007) 78–86.
[100] O. Houze, D. Viturat, O.S. Fjaere, Dynamic data analysis, Paris Kappa Eng. 694 (2008).
[101] A.A. Shchipanov, L. Kollbotn, R. Berenblyum, Characterization and monitoring of reservoir flow barriers from pressure transient analysis for CO2 injection in saline aquifers, Int. J. Greenh. Gas Control. 91 (2019), 102842, https://doi.org/10.1016/j.ijggc.2019.102842.
[102] T.A. Buscheck, Y. Sun, M. Chen, Y. Hao, T.J. Wolery, W.L. Bourcier, B. Court, M. A. Celia, S. Julio Friedmann, R.D. Aines, Active CO2 reservoir management for carbon storage: Analysis of operational strategies to relieve pressure buildup and improve injectivity, Int. J. Greenh. Gas Control. 6 (2012) 230–245, https://doi.org/10.1016/j.ijggc.2011.11.007.
[103] T.A. Buscheck, J.A. White, S.A. Carroll, J.M. Bielicki, R.D. Aines, Managing geologic CO2 storage with pre-injection brine production: a strategy evaluated with a model of CO2 injection at Snøhvit, Energy Environ. Sci. 9 (2016) 1504–1512, https://doi.org/10.1039/c5ee03648h.
[104] J.E. Heath, S.A. McKenna, T.A. Dewers, J.D. Roach, P.H. Kobos, Multiwell CO2 injectivity: impact of boundary conditions and brine extraction on geologic CO2 storage efficiency and pressure buildup, Environ. Sci. Technol. 48 (2014) 1067–1074.
[105] P.R. Neal, Y. Cinar, W.G. Allinson, The economics of pressure-relief with CO2 injection, Energy Procedia. 4 (2011) 4215–4220.
[106] P.R. Neal, Y. Cinar, W.G. Allinson, An integrated economic and engineering assessment of opportunities for CO2 injection with water production in South-East Queensland, Australia, Energy Procedia. 37 (2013) 4544–4551.
[107] F. Hussain, K. Michael, Y. Cinar, A numerical study of the effect of brine displaced from CO2 storage in a saline formation on groundwater, Greenh. Gases Sci. Technol. 6 (2016) 94–111.
[108] P. Newell, M.J. Martinez, P. Eichhubl, Impact of layer thickness and well orientation on caprock integrity for geologic carbon storage, J. Pet. Sci. Eng. 155 (2017) 100–108, https://doi.org/10.1016/j.petrol.2016.07.032.
[109] E.A. Al-Khdheeawi, S. Vialle, A. Barifcani, M. Sarmadivaleh, S. Iglauer, Influence of injection well configuration and rock wettability on CO2 plume behaviour and CO2 trapping capacity in heterogeneous reservoirs, J. Nat. Gas Sci. Eng. 43 (2017) 190–206, https://doi.org/10.1016/j.jngse.2017.03.016.
[110] M. Abdelaal, M. Zeidouni, I.J. Duncan, Effects of injection well operation conditions on CO2 storage capacity in deep saline aquifers, Greenh. Gases Sci. Technol. 11 (2021) 734–749, https://doi.org/10.1002/ghg.2076.
[111] J. Henninges, A. Liebscher, A. Bannach, W. Brandt, S. Hurter, S. Köhler, F. Möller, C. Group, PT-ρ and two-phase fluid conditions with inverted density profile in observation wells at the CO2 storage site at Ketzin (Germany), Energy Procedia. 4 (2011) 6085–6090.
[112] V. Vilarrasa, J. Carrera, D. Bolster, M. Dentz, Semianalytical Solution for CO2 Plume Shape and Pressure Evolution During CO2 injection in Deep Saline Formations, Transp. Porous Media. 97 (2013) 43–65.
[113] V. Vilarrasa, D. Bolster, S. Olivella, J. Carrera, Coupled hydromechanical modeling of CO2 sequestration in deep saline aquifers, Int. J. Greenh. Gas Control. 4 (2010) 910–919.
[114] J.T. Birkholzer, Q. Zhou, C.-F. Tsang, Large-scale impact of CO2 storage in deep saline aquifers: A sensitivity study on pressure response in stratified systems, Int. J. Greenh. Gas Control. 3 (2009) 181–194.
[115] Z. Zhang, R.K. Agarwal, Numerical simulation and optimization of CO2 sequestration in saline aquifers for vertical and horizontal well injection, Comput. Geosci. 16 (2012) 891–899.
[116] R.T. Okwen, M.T. Stewart, J.A. Cunningham, Temporal variations in near-wellbore pressures during CO2 injection in saline aquifers, Int. J. Greenh. Gas Control. 5 (2011) 1140–1148.
[117] W. Yu, H.R. Lashgari, K. Wu, K. Sepehrnoori, CO2 injection for enhanced oil recovery in Bakken tight oil reservoirs, Fuel. 159 (2015) 354–363, https://doi.org/10.1016/j.fuel.2015.06.092.
[118] L. Jin, S. Hawthorne, J. Sorensen, L. Pekot, B. Kurz, S. Smith, L. Heebink, V. Herdegen, N. Bosshart, J. Torres, C. Dalkhaa, K. Peterson, C. Gorecki, E. Steadman, J. Harju, Advancing CO2 enhanced oil recovery and storage in unconventional oil play—Experimental studies on Bakken shales, Appl. Energy. 208 (2017) 171–183, https://doi.org/10.1016/j.apenergy.2017.10.054.
[119] B. Jia, J.-S. Tsau, R. Barati, A review of the current progress of CO2 injection EOR and carbon storage in shale oil reservoirs, Fuel. 236 (2019) 404–427, https://doi.org/10.1016/j.fuel.2018.08.103.
[120] S.B. Hawthorne, C.B. Grabanski, L. Jin, N.W. Bosshart, D.J. Miller, Comparison of CO2 and Produced Gas Hydrocarbons to Recover Crude Oil from Williston Basin Shale and Mudrock Cores at 10.3, 17.2, and 34.5 MPa and 110 °C, Energy Fuels 35 (2021) 6658–6672, https://doi.org/10.1021/acs.energyfuels.1c00412.
[121] B. Ren, S. Ren, L. Zhang, G. Chen, H. Zhang, Monitoring on CO2 migration in a tight oil reservoir during CCS-EOR in Jilin Oilfield China, Energy 98 (2016) 108–121, https://doi.org/10.1016/j.energy.2016.01.028.

[122] R. Sander, L.D. Connell, M. Camilleri, Z. Pan, CH4, CO2, N2 diffusion in Bowen Basin (Australia) coal: relationship between sorption kinetics of coal core and crushed coal particles, J. Nat. Gas Sci. Eng. 81 (2020), 103468, https://doi.org/10.1016/j.jngse.2020.103468.

[123] M. Kazemi, A. Takbiri-Borujeni, Molecular Dynamics Study of Carbon Dioxide Storage in Carbon-Based Organic Nanopores, SPE Annu. Tech. Conf. Exhib. (2016) D011S009R006. doi: 10.2118/181705-MS.

[124] H. Pu, Y. Wang, Y. Li, How CO2-Storage Mechanisms Are Different in Organic Shale: Characterization and Simulation Studies, SPE J. 23 (2017) 661–671, https://doi.org/10.2118/180080-PA.

[125] H. Ansari, M. Trusler, G. Maitland, C. Delle Piane, R. Pini, The gas-in-place and CO2 storage capacity of shale reservoirs at subsurface conditions, in: Proc. 15th Greenh. Gas Control Technol. Conf., 2021: pp. 15–18.

[126] J.A. Sorensen, L.J. Pekot, J.A. Torres, L. Jin, S.B. Hawthorne, S.A. Smith, L. L. Jacobson, T.E. Doll, Field test of CO2 injection in a vertical middle Bakken well to evaluate the potential for enhanced oil recovery and CO2 storage, SPE/AAPG/SEG Unconv. Resour. Technol. Conf., OnePetro, in, 2018.